

Casting Defects Prediction from Solidification Simulation

Dissertation

*Submitted in the partial fulfillment of the requirements
for the degree of*

MASTER OF TECHNOLOGY
in
MECHANICAL ENGINEERING

Submitted by

Nilkanth R. Devshetwar

Roll. No. 98310026

Under the guidance of

Prof. B. Ravi



Department of Mechanical Engineering

Indian Institute of Technology-Bombay

January 2000

DISSERTATION APPROVAL SHEET

The dissertation entitled “Casting Defects Prediction from Solidification Simulation” by Nilkanth R. Devshetwar (Roll No. 98310026) has been approved for the degree of Master of Technology.

Guide

Chairman

Internal Examiner

External Examiner

ACKNOWLEDGEMENT

I sincerely express my deep gratitude for the valuable guidance and continuous encouragement I have received from my guide Prof. B.Ravi.

I am very much thankful to Dr. Giovanna Nicol, my tutor at Centro Ricerche Fiat Turin, Italy for her valuable suggestions and timely assistance for the completion of the project.

IIT BOMBAY

Jan. 2000

Nilkanth R. Devshetwar

[98310026]

CONTENTS

CHAPTER	TITLE	PAGE
	LIST OF FIGURES	
	LIST OF TABLES	
	NOMENCLATURE	
	ABSTRACT	
1	INTRODUCTION	... 1
	1.1 Casting Process	... 1
	1.2 Casting Solidification	... 1
	1.3 Solidification Simulation	... 2
2	PROBLEM DEFINITION	... 4
	2.1 Motivation	... 4
	2.2 Objectives	... 4
	2.3 Scope	... 5
3	LITERATURE REVIEW	... 6
	3.1 Governing Equations	... 6
	3.2 Shrinkage Prediction Methods	... 8
	3.2.1 Edge Function Approach	... 8
	3.2.2 Solid Fraction Approach	... 9
	3.2.3 Temperature Gradient Criteria	... 11
	3.2.4 Section Modulus Method	... 12
	3.2.5 Slicing Technique-3D	... 15
	3.2.6 Flux Vector Method	... 18
	3.3 Implementation Tools for Simulation	... 20
	3.3.1 Finite Difference Method	... 20
	3.3.2 Finite Element Method	... 21
	3.3.3 Boundary Element Method	... 24
	3.4 Summary of Literature Review	... 25

4	SOIDIFICATION SIMUATION SOFTWARE	... 26
4.1	Introduction	... 26
4.2	NovaSolid	... 26
4.2.1	Build Geometry	... 26
4.2.2	Initial Conditions	... 27
4.2.3	Simulation	... 27
4.2.4	Browse Results	... 30
4.2.5	Database	... 30
4.3	MAGMAsoft	... 31
4.3.1	Project management module	... 31
4.3.2	Preprocessor module	... 31
4.3.3	Mesh generator module	... 33
4.3.4	Mold filling module	... 33
4.3.5	Solidification module	... 34
4.3.6	Postprocessor module	... 34
4.3.7	Database module	... 35
4.4	PAMCAST/SIMULOR	... 37
4.4.1	Study	... 37
4.4.2	Surface Model	... 38
4.4.3	Volume Model	... 38
4.4.4	Data Assignment	... 39
4.4.5	Calculations	... 40
4.4.6	Results	... 41
4.4.7	Databases	... 41
4.5	Case Study for Comparison	... 41
5	DESIGN OF SIMULATION EXPERIMENTS	... 47
5.1	Preliminary Simulation Experiments	... 47
5.1.1	Casting Shape and Dimensions	... 48
5.1.2	Design of Experiments and Results of simulation	... 48
5.1.3	Discussion of Results and Conclusions	... 49
5.2	Simulation Experiments	... 54

	5.2.1	Material Details	... 54
	5.2.2	Critical Points in the Geometry	... 55
	5.2.3	Structure of Simulation Sheet	... 55
	5.2.4	Design of Experiments	... 57
6		SENSITIVITY ANALYSIS MODEL	... 59
	6.1	Introduction	... 59
	6.2	Weight assignment using AHP	... 59
	6.2	Basic Model	... 62
	6.3	Advanced Model	... 65
7		RESULTS AND ANALYSIS	... 71
	7.1	Results	... 71
	7.2	Conclusions	... 74
	7.3	Customization	... 76
8		CONCLUSIONS	... 78
	8.1	Summary of Work done	... 78
	8.2	Conclusions of Work done	... 78

REFERENCES

LIST OF FIGURES

FIG.	TITLE	PAGE
1.1	Typical architecture of a solidification modeling system	... 2
3.1	An idealized 2-D sand-casting system	... 8
3.2	Cross-section of a cavity with multiple corners	... 9
3.3	Molten metal fluid region and isolated unsolid region	... 10
3.4	Prediction of shrinkage cavity portion	... 11
3.5	(a) Solidification time and (b) Temperature gradient at the end of solidification of a ring casting	... 12
3.6	2-D Application of Chorinov's rule in square corner	... 13
3.7	Vantage point angles θ (j) from an internal point	... 13
3.8	Freezing wave fronts with rectangular cross sections	... 15
3.9	Infinite plate section	... 15
3.10	Model for k- contour development for external corners	... 16
3.11	R/10 contour for a thick semi-infinite plate	... 17
3.12	The slicing technique used to simulate 3-D shapes as 2-D slices	... 17
3.13	Isothermal contours and temperature gradient in casting section	... 18
3.14	Flux vector method for determining temperature gradient	... 18
3.15	Hot spot location	... 19
3.16	Adaptive remeshing in phase change region	... 24
3.17	Discretization of casting and mold	... 24
4.1	Picture of imported file in Build geometry module	... 28
4.2	Picture of Initial conditions module	... 28
4.3	Mesh, Temperature, Liquid fraction and Shrinkage Field	... 29
4.4	Shrinkage result saved in Browse results module	... 29
4.5	Constitution diagram for Grey iron in Database module	... 30
4.6	Picture of Project module of MAGMAsoft to open a project	... 32
4.7	Picture of MAGMApre for modeling a geometry	... 32
4.8	Picture of Mesh generation module	... 33
4.9	Picture showing filling definition for MAGMAfill module	... 34

4.10	Picture showing solidification definition for MAGMASolid module	... 35
4.11	Picture of MAGMApost module	... 36
4.12	Picture of MAGMAdata module	... 36
4.13	The picture of Study menu to create a new study	... 37
4.14	Import of CAD mesh in SIMULOR	... 38
4.15	Grid information in Volume Model	... 39
4.16	Definition of physical parameters for solidification	... 39
4.17	Parameters to run the solidification calculation	... 40
4.18	Predicted shrinkage result in a casting section	... 41
4.19	Picture of STL geometry used for the case study	... 43
4.20	Predicted results with NovaSolid (a) Shrinkage (b) Temperature distribution	... 44
4.21	Predicted results with MAGMASoft (a) Shrinkage (b) Temperature distribution	... 45
4.22	Predicted results with SIMULOR (a) Shrinkage (b) Temperature distribution	... 46
5.1	Middle section of the casting used for simulation	... 47
5.2	Picture of solid model prepared in ProEngineer	... 48
5.3	Porosity values along X-axis for different materials	... 51
5.4	Effect of length on porosity values along X-axis	... 52
5.5	Effect of fillet radius on porosity values along X-axis	... 52
5.6	Effect of width on porosity values along X-axis	... 53
5.7	Effect of pouring temperature on porosity values along X-axis	... 53
5.8	Critical points in the sample geometry (Section at the middle)	... 55
5.9	Simulation sheet to note the results of simulation	... 56
6.1	Flowchart showing the overall process of analysis	... 60
6.2	Typical picture of sheet 1 of basic model	... 62
6.3	Weight assignment to critical points using AHP	... 63
6.4	Picture showing result sheet of basic model	... 64
6.5	Flowchart of advanced model for sensitivity analysis	... 65

6.6	Picture showing sheet 1 of advanced model	... 66
6.7	Picture showing the sheet 2 of advanced model	... 67
6.8	AHP used to calculate average porosity for the superheat parameter	... 67
6.9	Input format for single valued result	... 68
6.10	Normalization of parameters	... 69
6.11	Graph to see the variations in between minimum and maximum value	... 69
6.12	Picture of sheet 7 showing results of analysis	... 70
7.1	Screen print of results with MAGMAsoft for the study object	... 72
7.2	Screen print of shrinkage result with SIMULOR for the study object	... 72
7.15	Proposed method for Customization	... 77

LIST OF TABLES

Table	Title	Page
4.1	Comparison of software package for the case study	... 42
5.1	Design of Experiments for NovaSolid	... 48
5.2	Structure of sensitivity analysis for NovaSolid.	... 49
5.3	Properties of material	... 54
5.4	Co-ordinates of critical points	... 55
5.5	Design of Experiments for MAGMAsoft	... 57
5.6	Design of Experiments for SIMULOR	... 57
5.7	Sensitivity analysis structure for MAGMAsoft	... 58
5.8	Sensitivity analysis structure for SIMULOR	... 58
6.1	Scale of relative importance	... 61
6.2	Random consistency Index table (RI)	... 61
7.1	Summary of results of basic model	... 73
7.2	Results from advanced model	... 74
7.3	Conclusions from the results of basic model	... 75
7.4	Conclusions from the results of advanced model	... 76

NOMENCLATURE

A	-	Area
a	-	Distance
C	-	Specific heat
c	-	Centroid
E	-	Edge function
F	-	Force vector
g	-	Flux vector
H	-	Enthalpy
h	-	Heat transfer coefficient
k	-	Thermal conductivity
L	-	Latent heat
l	-	Length
P	-	Perimeter
Q	-	Rate of internal heat generation
q	-	Heat flux
R	-	Thickness
r	-	Radius
T	-	Temperature
t	-	time
V	-	Volume
W	-	Width
α	-	Thermal diffusivity
β	-	Solid angle
γ	-	Coefficient of time step integration
λ	-	Eigen value

Subscripts

c	-	Casting
m	-	Mold
o	-	Ambient
cr	-	Critical
w	-	Mold wall

Abbreviations

AHP	-	Analytical Hierarchy Process
BEM	-	Boundary Element Method
C.L.E.	-	Coefficient of Linear Expansion
FDM	-	Finite Difference Method
FEM	-	Finite Element Method
SM	-	Section Modulus
SMMAX-	-	Maximum Section Modulus
1-D	-	One Dimension
2-D	-	Two Dimension
3-D	-	Three Dimension

ABSTRACT

Owing to increasing pressure to improve quality and to reduce cost, many foundries are exploring software packages, which help to reduce the need of trials and prototyping. However there is always a difference in actual and predicted location of defects, especially for new materials, shapes and processes. To correlate the actual and predicted location of defects, customization of software is necessary which is very expensive and time consuming.

This project deals with the study of various issues in solidification modeling of metal casting to identify critical parameters, which influence defect prediction followed by sensitivity analysis to enable customization of solidification software. Part of the project work was carried out at Centro Ricerche Fiat Turin, Italy.

The sensitivity analysis models were developed using Microsoft Excel. Critical parameters (sensitive and important) were identified for commercial casting simulation packages available at Centro Ricerche Fiat. Based on the study a systematic approach for the customization of given software was evolved.

CHAPTER 1

INTRODUCTION

1.1 Casting Process

Casting is one of the most economical method for obtaining near net shape parts in virtually any metal or alloy. Casting offers the following advantages compared to other processes:

Size Casting is the only method available for producing massive parts weighing several tones, as a single piece.

Complexity Complicated shapes that would otherwise be very difficult or impossible by other methods can be obtained.

Weight Saving As the metal can be placed exactly where it is required in part (features), large saving in weight is achieved.

Dimensional Accuracy Casting can be made to desirable dimensional tolerances by choosing the proper type of molding and casting process.

Versatility in Production Metal casting is adaptable to all types of production: automatic or manual, single piece or mass production, etc.

1.2 Casting Solidification

This is perhaps most important phenomenon during the production of cast component. Heat is extracted from molten metal as metal enters the mold. As metal cools from poured temperature to the room temperature, it involves three major heat transformations to complete the solidification: (1) Poured liquid metal transforms heat so as to start solidification of metal (2) Release of latent heat during solidification (3) Solidified metal transforms heat as it cools to room temperature. During the three stage of cooling: liquid, liquid-solid, and solid shrinkage is also occurring. Thus metal contracts as it loses superheat, as it transforms to solid and as the solid cools to room temperature. Additional variables which add to the complexity of the process include following:

- Alloy freezes over a range of temperature, and release of latent heat from a moving solid/liquid boundary.

- Presence of all three modes of heat transfer (conduction, convection, and radiation) are involved
- Varying thickness of air gap at the casting/mold interface and unavailability of exact heat transfer coefficient at the interface.
- Varying rates of heat transfer coefficient in different parts (like chills, cores) of mold.
- Intricate geometry of industrial casting.

Hence simulation of solidification process is important need to predict location of defects.

1.3 Solidification Simulation

Several software packages are available today to analyse the solidification behavior of complex shaped castings. These packages make use of different approaches to analyse the solidification process. These included in the next chapter.

For production of a sound casting, the exact location of hot spot at which shrinkage cavity is formed is necessary. Simulation analysis provides location of shrinkage defect with which one can design the feeder of optimum size. For large casting, produced in small number the cost of failure is very high. After analysing defect from simulations changes in the design can be made to eliminate the defect. Thus casting design can be corrected prior to molding on the basis of shrinkage prediction.

An overall architecture of a solidification modeling system is shown in Fig. 1.1 [1]. Typical inputs for solidification simulation include properties of material (metal and mold), boundary conditions depending on the process and rigging design (which is based on initial design and empirical rules). Solidification simulation program calculates time dependent temperature distribution, solid fraction, etc. inside the casting. The postprocessor takes inputs from simulated result and provides different result like grain size, dendrite arm spacing, macro and micro porosity, mushy zone formed and shrinkage stress distribution. Use of solidification simulation software packages for the industry offers benefits like:

- Increased yield of casting.
- Reduction in scrap and rework.
- Reduction in total manufacturing cost.

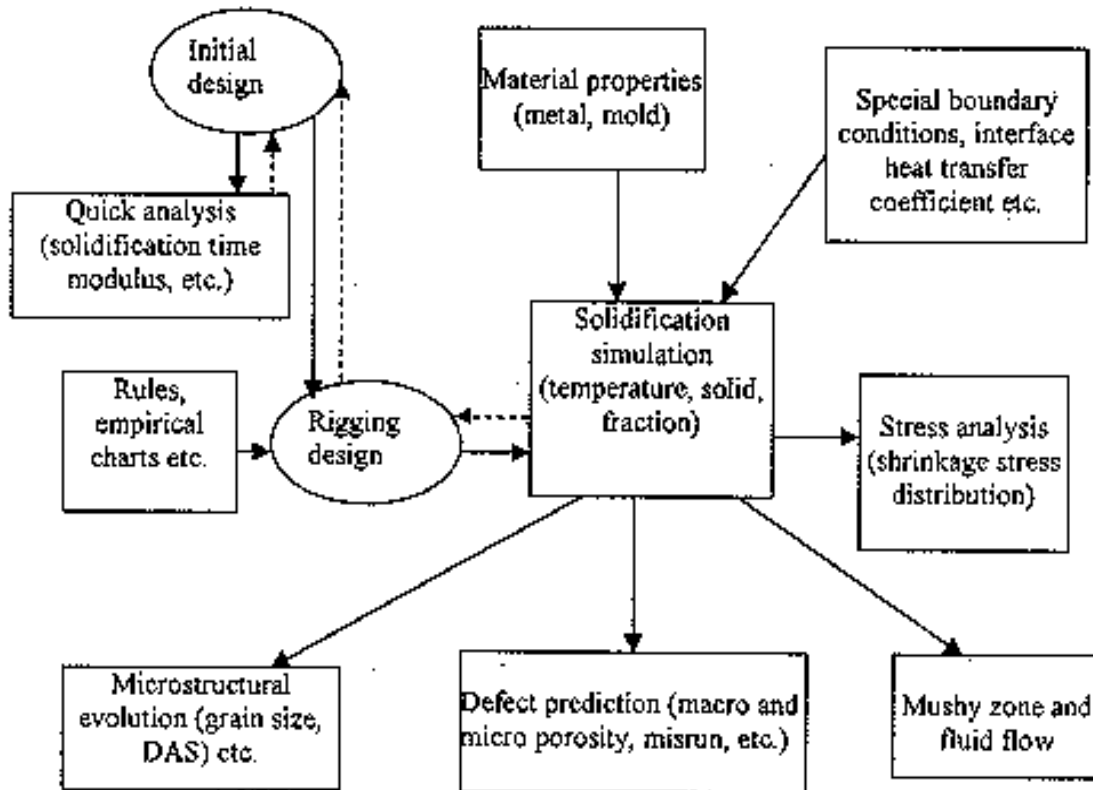


Fig. 1.1 Typical architecture of a solidification modeling system [1].

- Reduction in lead time.
- Improved quality of casting.
- Quick assessments in daily use.
- Highly visual results for easier communication with customer.
- Customer satisfaction.

In spite of these benefits, solidification simulation has limitations, as there is always a difference in actual and predicted location of defects. This is because the software needs extensive customization for a particular casting industry depending on materials, processes, equipment and other conditions to match predicted results with actual results. This project attempts to explore a systematic methodology for customizing solidification software based on sensitivity analysis of important parameters affecting the results.

CHAPTER 2

PROBLEM DEFINITION

2.1 Motivation

In recent years, significant strides have been made in the field of solidification modeling of casting by means of computer simulation. One can experiment with riser size and placement, chills, sleeves, mold materials and different alloys on computer screen before making a single casting and that too in much less time. However these software packages need extensive customization in a particular company through a series of trials to compare the predicted and actual location of defects. This is because the large number of parameters, material properties and process variables affect the prediction of casting defects. This exercise of customization requires technical expertise and can take several weeks to months.

2.2 Objectives

Objectives of this project are:

- Study various issues of solidification modeling and capabilities of commercial software packages.
- Identify critical parameters influencing the results of simulations.
- Evolve a systematic approach to study the effect of critical parameters, to enable customization of software.

3.3 Scope

The project scope is limited to the following:

Process : Sand casting

Defect : Shrinkage

Materials : Carbon steel, Aluminum alloys

Instantaneous filling (suitable for thick section casting).

3.4 Approach

The literature on heat transfer analysis of casting process, shrinkage prediction methods and the numerical methods was reviewed. User interface of commercial software packages NovaSolid, MAGMAsoft and SIMULOR made available for the project were studied. Sensitivity analysis models were developed using Microsoft Excel. Critical (sensitive and important) parameters were identified for MAGMAsoft and SIMULOR. At the end, a systematic approach for customization of simulation software for given organization was evolved.

CHAPTER 3

LITERATURE REVIEW

3.1 Governing Equations

Numerical simulation of solidification process requires following steps [2]:

- Formulating an accurate physical description of the casting and solidification process in the mathematical form.
- Use of accurate values for thermal properties of the materials involved.
- Performing a suitable numerical analysis (either FEM or FDM based) to obtain temperature relationships at specified space co-ordinates in the casting and mold, so as to predict shrinkage defects.

For solidification simulation of the casting several assumptions are usually made, these include:

- The filling is instantaneous, that is solidification starts after complete filling.
- The liquidus and solidus temperature are well defined, so that plotting of beginning of freeze and end of freeze curve is possible.
- Only one mode of heat transfer (conduction) is assumed, whereas all three modes (conduction, convection and radiation) are present in actual solidification process.

Governing equation for solidification of casting is given by [3],

$$\rho \cdot C \frac{\partial T}{\partial t} = \nabla \cdot K \nabla T + \dot{Q} \quad \dots(3.1)$$

Where, C - specific heat,

K - thermal conductivity,

T - temperature,

ρ - density,

\dot{Q} - rate of internal heat generation,

t - time.

Heat generated (assuming that latent heat is released at the rate of formation of the solid fraction f_s) in casting is given by,

$$\dot{Q} = L \frac{d f_s}{dt} \quad \dots(3.2)$$

Where, L - total latent heat, f_s - solid fraction ratio, t - time.

Boundary conditions

For solving governing equation (3.1) boundary conditions are necessary. In solidification simulation, generally following three types of boundary conditions are used:

(1) Specified Temperature

In this type the temperature at the boundary is specified. Marrone et.al assumed that temperature at the outside mold wall is constant, $T_w = 30^\circ\text{C}$ (where T_w is mold wall temperature) [4]. Majchrzak and Mendakiewicz assumed same temperature between casting and mold [5].

$$T_c \left[H_c(x, t) \right] = T_m(x, t) \quad \dots(3.3)$$

Where, x - Spatial co-ordinate,

t - Time co-ordinate,

T_c - Temperature of the casting at the interface,

T_m - Temperature of the mold at the interface,

H_c - Enthalpy of casting.

(2) Specified Heat Flux [4]

In this type heat flux at the boundary is specified. Continuity of heat flux across the sand-metal interface gives,

$$K_c \frac{\partial T_c}{\partial n} = K_m \frac{\partial T_m}{\partial n} \quad \dots(3.4)$$

Where, n - co-ordinate normal to the sand-metal interface,

T - temperature.

Subscripts c and m are for casting and mold.

(3) Convection Type[1]

Heat loss at the boundary is expressed in terms of heat transfer coefficient:

$$q = -K \left. \frac{dT}{dx} \right|_{x=bound} = h(T - T_o) \quad \dots(3.5)$$

Where, q - heat flux,

h - interface heat transfer coefficient,

T_o - ambient temperature, x - spatial co-ordinate.

3.2 Shrinkage Prediction Methods

The first three methods described in this section are based on heat transfer approach. This approach gives detailed thermal analysis of solidification, but require large computational time. The last three methods described in this section are geometry driven methods, which offer the advantage of being faster and less dependent on material properties than heat transfer approaches.

3.2.1 Edge Function Approach

For the simulation of sand casting system mold space involved is divided into small volume elements so as to use finite difference or finite element analysis. Since sand molds are much larger in size than casting, 70-80% of the volume elements are located in the mold. The temperature inside the mold is not important, so heat dissipation into the mold is represented by heat transfer coefficient. This approach gives a general form for the effective heat transfer coefficient at mold casting interfaces, which in effect eliminate the need to compute the temperature field within sand molds [6]. The mold is treated as an isolated enclosure subjected to an isothermal heat source at cavity wall. Isothermal heat source can be assumed because there is release of latent heat from the molten metal, which keep uniform temperature at the mold-casting interface. With the assumption that mold is initially at zero temperature and isothermal heat source at the cavity wall is at a unit temperature it has been shown that the heat flux per unit time per unit area at the surface of the mold enclosure $q(r,t)$ is the product of one dimensional corner free surface heat flux and an edge function (E-function) that is dependent only on Fourier number. This method for simulation is known as q-method (Fig. 3.1).

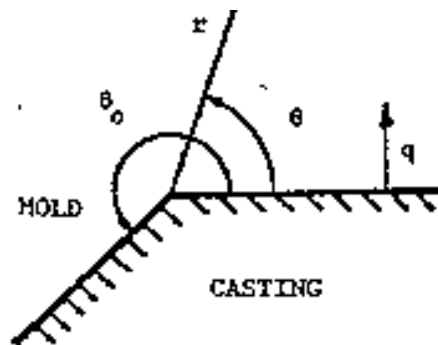


Fig. 3.1 An idealized 2-D sand casting system [6].

$$q_{(r,t)} = q_{1-d}(t) \cdot E_{\theta}(F_o) \quad \dots(3.6)$$

Where, q_{1-d} - heat flux in one dimension ($K/\pi\alpha t$) , t - time,
 K - thermal conductivity, E_{θ} - edge function,
 α - thermal diffusivity, F_o - Fourier number.

For a two dimensional shape the heat flow rate is given by (Fig. 3.2),

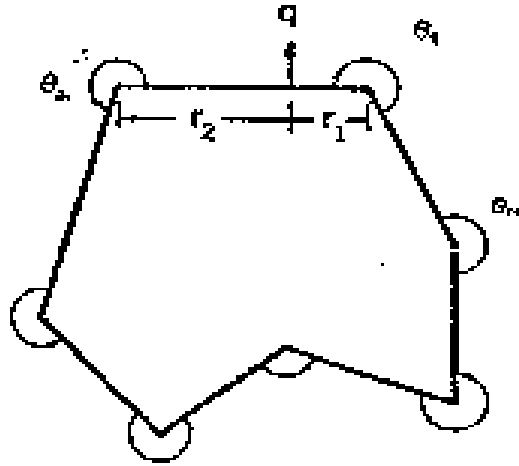


Fig. 3.2 Cross-section of a cavity with multiple corners [6].

$$q = q_{1-d} \left[E_{\theta_1} \left(\frac{r_1}{2\sqrt{\alpha t}} \right) + E_{\theta_2} \left(\frac{r_2}{2\sqrt{\alpha t}} \right) - 1 \right] \quad \dots(3.7)$$

Using above equation, value of h is approximated as:

$$h = \frac{K_m}{\sqrt{\pi \alpha_m t}} \left[E_{\theta_1} \left(\frac{r_1}{2\sqrt{\alpha_m t}} \right) + E_{\theta_2} \left(\frac{r_2}{2\sqrt{\alpha_m t}} \right) - 1 \right] \quad \dots(3.8)$$

Where, h - hypothetical heat transfer coefficient.

Subscripts 1 and 2 represent the neighboring corners.

Using the hypothetical heat transfer coefficient acting at mold-metal interface solidification time contours can be obtained from which shrinkage cavity can be predicted.

3.2.2 Solid Fraction Approach [7]

This method for prediction of shrinkage cavities is based on cavity generation mechanism. Shape of the shrinkage cavity is analytically formulated as the function of

solid fraction and shrinkage cavity ratio. Following assumptions were made in the analysis [7].

- 1) Molten metal moves downward with the force of gravity
- 2) The moving speed of the molten metal is far greater than that of the solidification
- 3) The volume of shrinkage cavity is equal to the volume of contraction by solidification
- 4) Molten metal has full fluidity in a solid-liquid region where the solid fraction ratio is less than f_{cr} (critical fluid solid fraction ratio).

During phase change of molten metal latent heat is released. This heat released is proportional to the rate of solid fraction. The solid liquid region is divided into two subregions p and q. In the p subregion the fluidity of the molten metal within the dendrite structure does not exist, however the molten metal in the q subregion can move downwards by the force of gravity. Then solid fraction ratio at the boundary p and q subregions is defined as the fluid critical solid fraction ratio (f_{cr}). Figure 3.3 shows relation between molten metal fluid region and isolated un-solid region. Fluidity will be there within f_{cr} loop so, after small time interval the molten metal moves in the downward direction and the shrinkage cavity, which has same volume as the solidification shrinkage

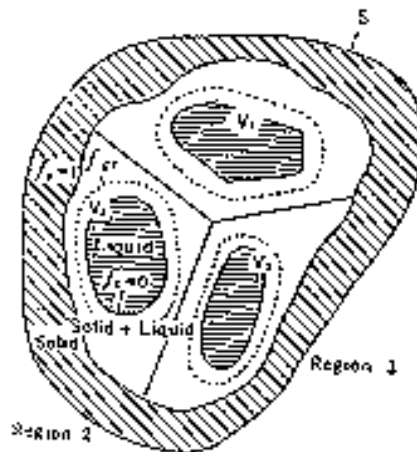


Fig. 3.3 Molten metal fluid region and isolated un-solid region [7].

which is generated at the upper part of the f_{cr} loop. So shape of shrinkage cavity depend on the previously generated shrinkage cavity, the shape of the f_{cr} loop, and the volume of the generated shrinkage cavity. Figure 3.4 shows a prediction of shrinkage cavity portion.

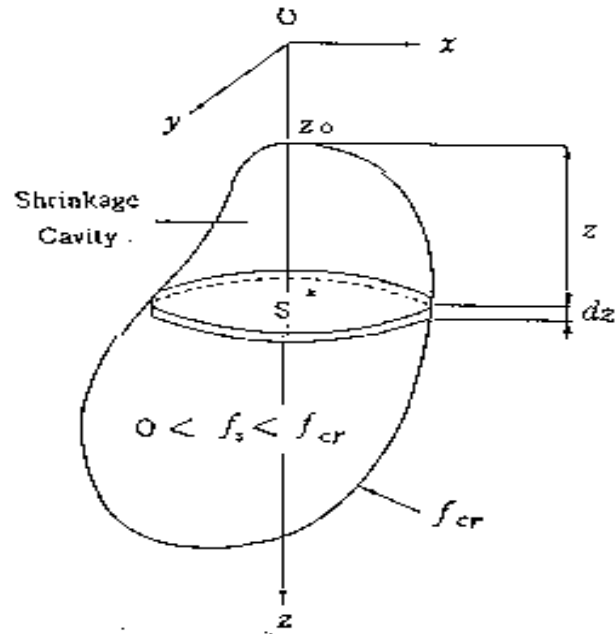


Fig. 3.4 Prediction of shrinkage cavity portion [7].

The coordinate of the highest point of the molten metal fluid region is defined as z_0 and z axis is in the downward direction. dz is the thin plate perpendicular to the z -axis, as the plate is thin the volume ratios of solid, liquid, solid-liquid and shrinkage cavities are constant in the z -direction. New shrinkage cavity formed will be at the top of the fluid region as molten metal moves downwards by the force of gravity. Thus shrinkage cavity for each loop is predicted. The whole casting is analysed by FEM. Formulation is done for enthalpy H which is function of solid fraction ratio [7]. Thus shrinkage cavity can be predicted within the f_{cr} loop.

3.2.3 Temperature Gradient Criteria

In shrinkage prediction methods discussed so far shrinkage is assumed to be occurring at isolated hotspot. Temperature gradient criterion is a powerful tool for predicting centerline shrinkage defect [8].

Solidification starts at the middle section and ends in the thick sections, which are at the end (Fig. 3.5a). So expected shrinkage areas are in thick sections. However actual ultrasonic examination shows that shrinkage occurs in the middle (Fig. 3.5 b).

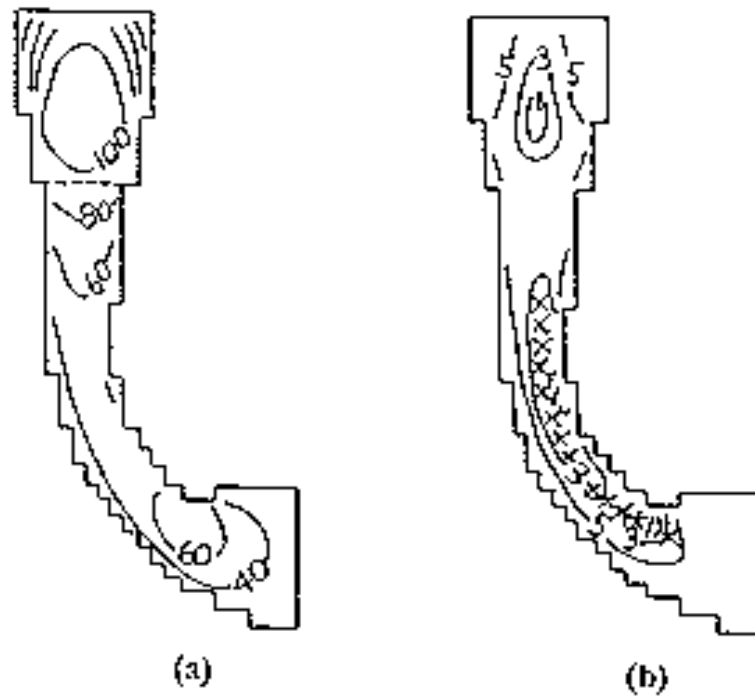


Fig. 3.5 (a) Solidification time and (b) Temperature gradient at the end of solidification of a ring casting [8] (X indicates shrinkage).

Niyama et.al concluded that the region of low temperature gradient coincide with the location of such shrinkage [8].

For calculation of temperature gradient, he suggested the following method. The temperature θ_0 of the element at time t changes to θ'_0 after a time increment Δt and passes the solidus of the alloy during Δt . Temperature gradients at $t + \Delta t$ from the centrepoint to the eight surrounding points are examined and the maximum positive value among them is taken as the temperature gradient G at the end point of the solidification point. This is the path for the ease of liquid metal feeding for the solidification shrinkage at that point. So as to avoid centerline shrinkage the value of G should be greater than critical temperature gradient, the value of which depend on casting type, alloy composition, sensitivity of inspection.

3.2.4 Section Modulus Method

Neises et.al explained section modulus method for directional solidification modeling of casting [9]. The basis of this method is Chrorinov's rule, which is given by:

$$\log t = k \log (V / A) + b \quad \dots(3.9)$$

Where, V - total casting volume,
 A - total surface area,
 t - total solidification time,
 b,k - constants.

Equation (3.9) gives total solidification time if section modulus or (V/A) ratio is known. Since the end of solidification is considered the coarse of solidification that is beginning, intermediate and end stages are not expressed by equation (3.9).

Neises et.al gave the section modulus principle to depict the direction and endpoint of solidification. They considered basic two-dimensional cross sections such as circles, squares, polygon etc. rather than a complete casting volume. And for 2-D the section modulus (SM) is modified as follows.

$$SM = \frac{V}{A} = \frac{A}{P} \quad \dots(3.10)$$

Where, V - volume, A - area, P - perimeter.

Now for Fig. 3.6,

Cross-sectional area of corner = (X, Y)

External perimeter of corner = X + Y

$$Section\ Modulus = \frac{A}{P} = \frac{XY}{X+Y} = \frac{1}{\frac{1}{X} + \frac{1}{Y}} \quad \dots(3.11)$$

Where, X and Y are perpendicular distances from a point to the nearest surface.

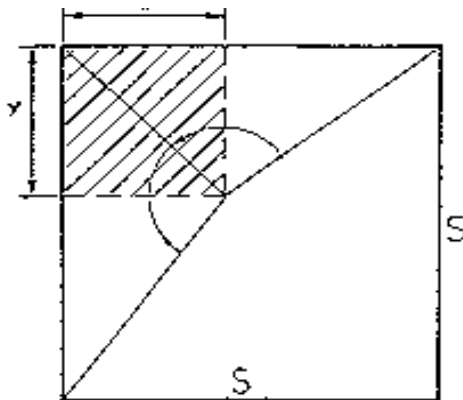


Fig. 3.6 2-D Application of Chorinov's rule in square corner [9].

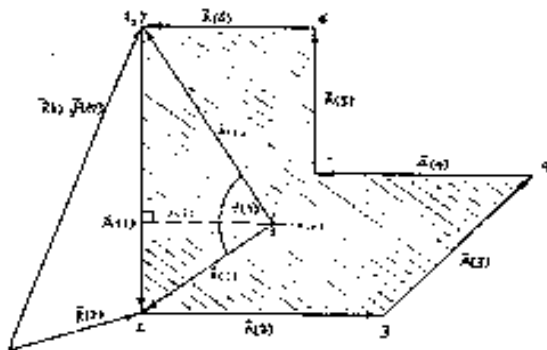


Fig. 3.7 Vantage point angles $\theta (j)$ from an internal point [9].

It can be observed that as X and Y increases, section modulus increases and solidification time required increases. So these X and Y are called geometrical parameters, which governs the section modulus or solidification time at that point. Neises et. al gave the relation between section modulus and geometrical parameters for a polygon with N edges (Fig. 3.7).

$$SM = \frac{A}{P} = \frac{1}{\sum_{j=1}^N \left[\frac{\theta(j)}{\pi} \cdot \frac{1}{a(j)} \right]} \quad \dots(3.12)$$

Where, a(j) - distance from a point to side j of the polygon,
 $\theta(j)$ - vantage point angle.

Vantage point angle determined by geometric information (Fig. 3.7). This angle may be defined as included angle formed when a pairs of vectors are drawn to the two endpoints of the edge (j) under consideration from a point inside the polygon. Application of equation (3.12) for a square crosssection with side S and (X, Y) vantage point at center gives,

$$\frac{A}{P} = \frac{1}{\frac{4(\pi/2)}{\pi} \cdot \frac{1}{S/2}} = S/4$$

Equation (3.12) is applicable for circular hole or equilateral triangle. For rectangular cross section normalization of the values calculated from equation (3.13) is done as:

$$\text{Modified } SM = \frac{A}{P} = \frac{1}{\sum_{j=1}^N \left[\frac{\theta(j)}{\pi} \cdot \frac{1}{a(j)} \right]} \left[\frac{A/P}{SM_{MAX}} \right] \quad \dots(3.13)$$

Where, SM_{MAX} - maximum value of A/P as determined from equation (3.10),
A/P - overall A/P ratio for the entire cross section.

Thus using equation (3.12) and (3.13) the section modulus at each point is determined and joining the point of same section modulus, contours can be obtained which are nothing but the solidification contours.

Figure 3.8 gives the results obtained by this method. Thus Neises et.al gave the general case equation and technique will clearly show the location and extent of shrinkage. However this method is applicable for 2-Dimensional analysis.

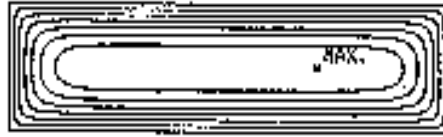


Fig. 3.8 Freezing wavefronts with rectangular cross sections [9].

3.2.5 Slicing Technique 3-D

This method gives a three dimensional solidification analysis, which is less costly than FEM, FDM, or classical heat transfer techniques by avoiding rigorous mathematical calculations. This technique can be used to provide approximated solution to the three dimensional problem using heat transfer approaches. Similar to the last method this technique is also based on casting modulus. This approach does not require all the physical properties of metal and mold. This method contains fewer and less complex mathematical relationships. The actual solidification time of the entire casting cannot be determined but this time is not important if we can obtain solidification sequence at various casting sequences.

Kotschi and Plutshack gave a method to obtain the casting modulus at various depths from the casting surface to the center of the plate [10]. For Fig. 3.9 which is infinite plate section,

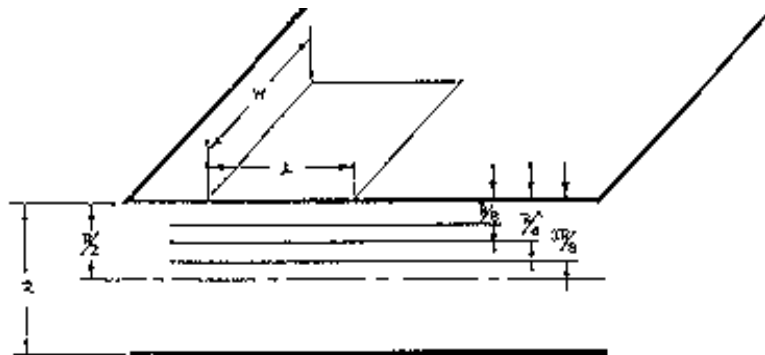


Fig. 3.9 Infinite plate section [10].

$$\text{Casting modulus} = \frac{V}{A} = \frac{lW \Delta R}{lW} = \Delta R \quad \dots(3.14)$$

Where, ΔR - distance from the plate surface to the depth of interest.

As ΔR varies from 0 at the surface to $R/2$ at the centerline casting modulus is 0 at the surface and $R/2$ at the centerline showing that solidification start at surface and ends

at center. Thus lines of casting modulus are obtained and technique is known as k-contour technique. In actual practice complex geometry of the casting is divided into simple components such as “L”, “T”, and “X” sections for calculations.

For the use of k-contour technique the type of corners encountered in two dimensional sections are important. For external corners the metal occupies the space whose angle of juncture is less than 180°. For internal corners the metal occupies the space whose angle of juncture is greater than 180°. Figure 3.10 shows the model for k-contour development for external corners.

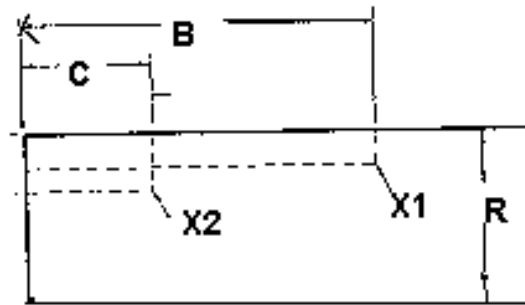


Fig. 3.10 Model for k-contour development for external corners [10].

Determination of X_1 on the R/10 contour:

$$\frac{V}{A} = \frac{R}{10} = \frac{C(R/X_1)}{C + (R/X_1)} \quad \dots(3.15)$$

$$X_1 = 10 - \frac{R}{C} \quad \dots(3.16)$$

$$X_2 = 10 - R/B \quad \dots(3.17)$$

Thus different points are plotted and Fig. 3.11 is obtained for T/10 contour. Similarly k-contours for L section can be obtained [10]. The importance of contours lies in analysis of 3-Dimensional shape. Kotschi and Plutshack have explained method to obtain 3-Dimensional solution from 2-D solutions.

For symmetrical object by determining the solidification sequence of the two dimensional slice passing through the center line, the three dimensional solution can be obtained by rotation. Figure 3.12 shows an object in which slices are taken and solidification contours are obtained for each slice. And then joining the contours having same value (isocontours), for all slices 3-Dimensional solution is obtained.

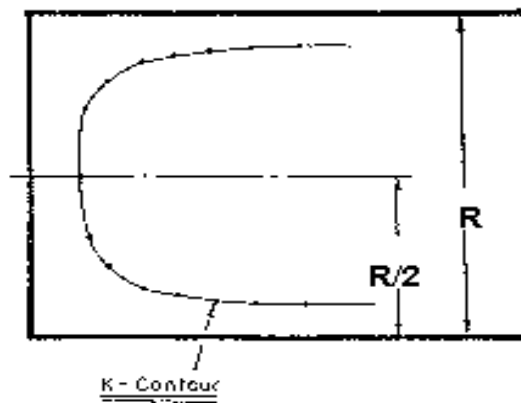


Fig. 3.11 R/10 contour for a thick semi-infinite plate [10].

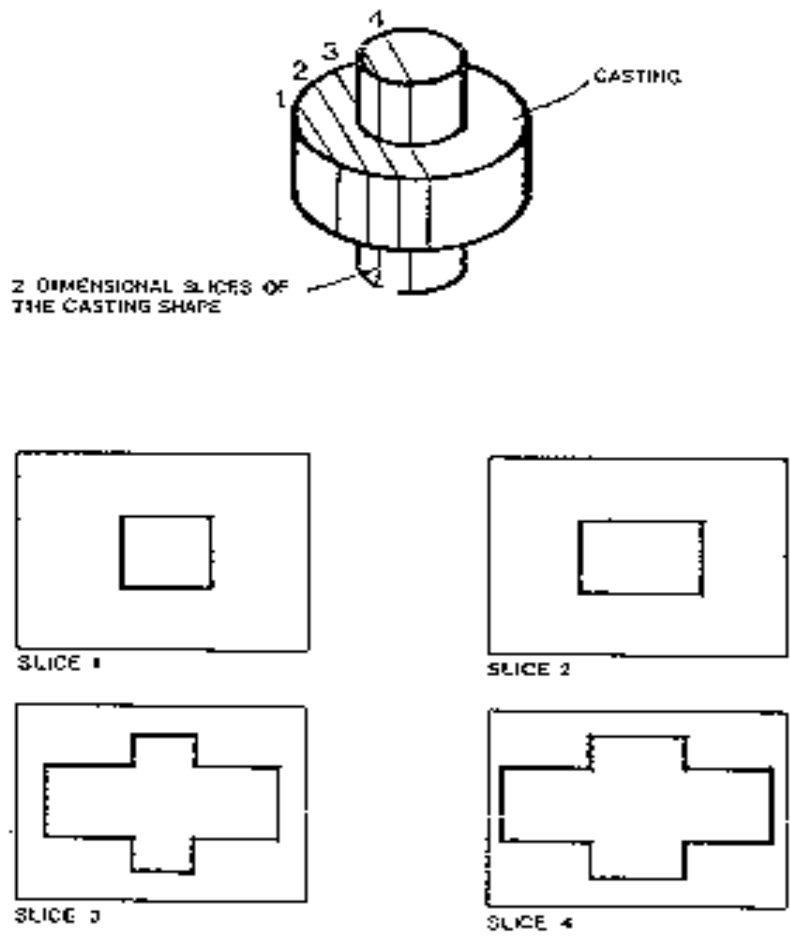


Fig. 3.12 The slicing technique used to simulate 3-D shapes as 2-D slices [10].

3.2.6 Flux Vector Method

Ravi and Srinivasan described a method to detect hot spot location as well as to find feeding path [11]. Another method for two dimensional casting section described by Ravi and Srinivasan is based on the principle that the flux vector is zero at the hot spot of a freezing section [12].

Basis of hot spot location is shown in Fig. 3.13. At point p_i on contour T_i , G_i represents the largest temperature gradient vector, the direction of which is normal to T_i at p_i . The intersection of this vector with next isothermal contour T_{i+1} gives point p_{i+1} . Now noting that p_{i+1} has higher temperature than p_i , p_{i+1} freezes after p_i and p_{i+1} is the nearest location to p_i so during solidification this is point which supply liquid metal so as to compensate for solidification shrinkage.



Fig. 3.13 Isothermal contours and temperature gradient in casting section [11].

Similarly proceeding for p_{i+2} , p_{i+3}, \dots, p_n . And last point gives the location of hot spot and path connecting $p_n, p_{n-1}, \dots, p_{i+1}, p_i$ gives feeding path. For locating hot spot actual values of T_i or T_{i+1}, \dots, T_n are not required. A modified method for 3-dimensional casting that determines the largest temperature gradient at any point inside the casting is described by Ravi and Srinivasan [11].

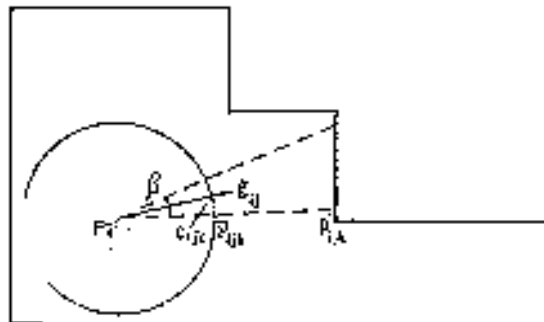


Fig. 3.14 Flux vector method for determining temperature gradient [11].

p_i is point inside the casting (Fig. 3.14). A unit sphere is constructed around the point p_i . Surface of sphere is then divided into n number of equal regular polygons. Then the flux vector \bar{g}_{ij} for this polygon is defined by [11].

$$\bar{g}_{ij} = \frac{3 \beta V_{ij}}{2\pi A_{ij}} (\bar{c}_{ijk} - \bar{p}_i) \quad \dots(3.18)$$

Where, \bar{c}_{ijk} - position vector of centroid of the polygon under consideration,

β - solid angle subtended by the polygon at the p_i ,

V_{ij} - volume of the pyramidal segment formed by extending rays from edges of polygon to the casting surface and apex of p_i ,

A_{ij} - base area of the pyramidal segments,

i - iteration number,

j - polygon number,

k - number of points on the sphere to form polygon.

This flux vector is modified by applying a factor known as modulus factor f_i , which considers the effect of presence of cores, re-extract corners in the mold, chills, insulating or isothermic materials, on the progress of solidification fronts. A detailed description and determination for f_i is described by Ravi and Srinivasan [11].

$$\bar{g}_{ij} = f_i \frac{3\beta \cdot V_{ij}}{2\pi A_{ij}} (\bar{c}_{ijk} - \bar{p}_i) \quad \dots(3.19)$$

Flux vector for all segments is,

$$\bar{G}_i = \sum_{j=1} \bar{g}_{ij} \quad \dots(3.20)$$

Location for next iteration will be,

$$\bar{p}_{i+1} = \bar{p}_i + \bar{G}_i \quad \dots(3.21)$$

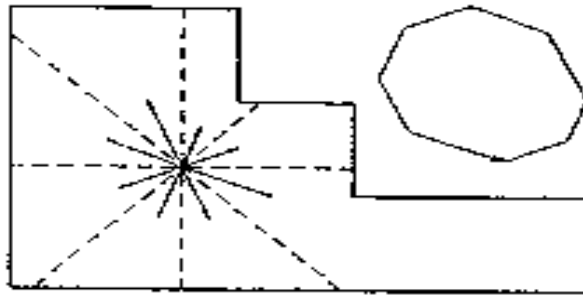


Fig. 3.15 Hot spot location [11].

Iterations are continued till the required accuracy is obtained. At the hot spot the value of G_i should be nearly zero. Fig. 3.15 explains flux vector method to obtain location of hot spot for a 2-Dimensional section. The section is divided into number of wedges and flux vector for a j th wedge.

$$\bar{g}_{ij} = \frac{2\beta A_{ij}}{\pi l_{ij}} (\bar{c}_{ij} - \bar{p}_{ij}) \quad \dots(3.22)$$

Where, β - angle of each wedge,

L_{ij} - length of its heat transmitting portion,

A_{ij} - wedge area.

Hot spot is located where, $\sum_{j=1}^n \bar{g}_{ij} = 0$

3.3 Implementation Tools for Simulation

This section describes different numerical tools implemented for solidification simulation such as finite difference method, finite element method and boundary element method.

3.3.1 Finite difference method

Complex heat transfer equations are solved by finite difference equation instead of partial differential equation. Time and space are discretized in small steps Δt , Δx , Δy , respectively. Method can be described as follows [13]. A series of horizontal and vertical lines equally spaced by Δx in x -direction, and Δy in y -direction are introduced throughout sand and metal. The intersection of these lines gives an array of grid points, each can be identified by subscripts i, j in the x, y -direction. At $t = 0$, the temperature at each grid point is obtained from initial condition. Let T_{ijn} denote the temperature computed at grid point (i, j) at a time $t_n = n\Delta t$. Each derivative of the equation and boundary condition is approximated by a suitable finite difference expression involving Δx or Δt , physical properties and T_{ijn} . This leads a set of algebraic equations in the T_{ijn} whose values may be computed over successive time interval. The accuracy will depend on values of Δx and

Δt . One dimensional cooling problem is governed by following partial differential equation [13].

$$\rho C_p \frac{\partial T}{\partial t} = k \frac{\partial^2 T}{\partial x^2} \quad \dots(3.23)$$

A finite difference equation [13] for any general grid point in the mold or casting is:

$$\rho C_p \left[\frac{T_{i,n+1} - T_{i,n}}{\Delta t} \right] = k \cdot \left[\frac{T_{i-1,n+1} - 2 T_{i,n+1} + T_{i+1,n+1}}{\Delta x^2} \right] \quad \dots(3.24)$$

3.3.2 Finite Element Method

For solving governing equation (3.1) of casting solidification, finite element method involves two major steps:

(1) *Spatial Discretisation*

Casting and mold domain is divided into elements. Finite element method is a method of piecewise approximation in which the approximating function is formed by connecting simple functions each defined over a small region (element). The mesh can mix elements of different types and shapes, one has to decide the shapes and sizes of the elements to achieve the required accuracy. Very small size leads to large computational time and large size of the element introduces errors in the results. A finite element is a region in space in which the approximation function is interpolated from nodal values of approximation function on the boundary of region in such a way that inter element continuity of approximation function tends to be maintained in the assemblage.

Thus, temperature T is approximated over each element in terms of total values by shape function as [14]:

$$T_e = \sum_{i=1}^n N_i T_i \quad \dots(3.25)$$

Where, T_e - temperature of element,

n - number of nodes in element,

N - shape function for temperature interpolation.

The governing equation (3.1) and boundary conditions are then approximated using above shape function. Lewis et.al using shape function approximation and

Newmann boundary condition obtained final set of spatially discretized equations in a fully coupled form [15].

$$M \dot{T} + K T = F \quad \dots(3.26)$$

Where, M - mass matrix, K - stiffness matrix,
F - force vector, T - temperature.

(2) Temporal Discretization

As the temperature is time dependent, a time varying solution may be obtained by the modal method or by direct temporal integration. If material properties are not temperature-dependent and the solution is dominated by a few of the lowest eigenmodes and needed over a long time span then the modal method is used. If the problem is nonlinear, or the solution displays sharp transients (which require many eigenmodes for an accurate description) and is needed over a time span then direct integration is favoured. Lewis et.al followed this by time integration. T_n and T_{n+1} are two temperature steps separated by time increment Δt . Then equation (3.26) becomes:

$$M (T_{n+\gamma}, t_{n+\gamma}) \dot{T}_{n+\gamma} + K (T_{n+\gamma}, t_{n+\gamma}) T_{n+\gamma} = F(T_{n+\gamma}, t_{n+\gamma}) \quad \dots(3.27)$$

Where, n- time step number, γ - coefficient for time integration.

Relation between two temperature steps and between two time steps is:

$$T_{n+\gamma} = (1 - \gamma) T_n + \gamma T_{n+1} \quad \dots(3.28)$$

$$\dot{T}_{n+\gamma} = \frac{T_{n+1} - T_n}{\Delta t} \quad \dots(3.29)$$

$$t_{n+\gamma} = t_n + \gamma \Delta t \quad \dots(3.30)$$

Using equations (3.27) to (3.30)

$$[M_{n+\gamma} + \gamma \Delta t K_{n+\gamma}] T_{n+1} = [M_{n+\gamma} - (1 - \gamma) \Delta t K_{n+\gamma}] T_n + \Delta t F_{n+\gamma} \quad \dots(3.31)$$

Depending on γ , time step Δt in equation (3.31) may have an upper limit if the algorithm is to be numerically stable [14]. If $\alpha < 1/2$ then the largest Δt for stability is given by:

$$\Delta t_{cr} = \frac{2}{(1 - 2\gamma) \lambda_{\max}} \quad \dots(3.32)$$

Where, λ_{\max} -largest eigenvalue.

If $\gamma \geq 1/2$ the algorithm is unconditionally stable that is stability is guaranteed (as Δt becomes indefinitely large). Names associated with various schemes are as follows,

$\gamma = 0$ Forward difference or Euler (conditionally stable)

$\gamma = 1/2$ Crank – Nicolson or Trapezoidal rule (unconditionally stable)

$\gamma = 2/3$ Galerkin (unconditionally stable)

$\gamma = 1$ Backward difference (unconditionally stable).

If $\gamma = 0$, algorithm is explicit, the computational effort per time step is small but largest Δt for stability is also small. If $\gamma > 0$, algorithm is implicit. Among implicit methods the choice $\gamma = 1/2$ is popular but sharp transients may excite annoying oscillations in the solution. Oscillations can be reduced by using a smaller value of Δt or numerically damped by using a value of γ somewhat greater than $1/2$. For the nonlinear problem only unconditionally stable form of equation (3.27) is $\gamma = 1$.

Thus implicit methods are economically attractive only when Δt can be much larger than that used in an explicit method. Unconditional stability coupled with the economic need for large Δt , tempts many analyst into using time steps that are too large.

Adaptive remeshing in phase change region

A very fine mesh is required in the region where the temperatures lie between solidus and liquidus values. Lewis et.al used adaptive remeshing technique for solidification simulation [15]. After solving the governing equation at a certain time step, a scan is made to determine all nodal points at which the phase change is occurring. Remeshing is then to produce a refined mesh only around these points (Fig. 3.16). The transformation of information from one solution to another is conducted as:

$$T_i^{n+1} = \sum_{j=1}^m N_j T_j^n \quad \dots(3.33)$$

Where, N - interpolation function, m - represents the nodes, n - time steps.

Finite element method offers some advantages over finite difference method. FEM gives better geometry description. Curved surfaces are well described by FEM, where as with FDM a stepwise shape should be used. Thin sections and complex shapes can only be accurately modeled using FEM with a reasonable number of elements. Moreover, if a local refinement of the mesh is required, it is not needed to propagate this

refinement all through the model, as it is the case with FDM. Thus number of nodes or elements can be kept much smaller with FEM than with FDM.

However the FDM is a little simpler on a numerical point of view and thus a larger number of elements can be handled with reasonable CPU times. However the required RAM memory in this case is very important because the result files are huge and take very long time to process. Moreover, because a lot of elements are required to ensure an acceptable geometry definition, CPU time saving becomes negligible.

3.3.3 Boundary Element Method

With the increase in complexity of the shape, numerical simulation of casting solidification requires large amount of time. So as to reduce the computational time combined FEM and BEM has been suggested [5,16].

Casting domain constitutes main part of the analysis. However heat transfer process in mold domain is very essential for the course of solidification. Hence casting can be modeled using FEM and mold region can be modeled using BEM. Coupling for two regions is then done using exponential function extrapolation/interpolation method. This approach essentially decreases the number of unknown parameters in considered mold.

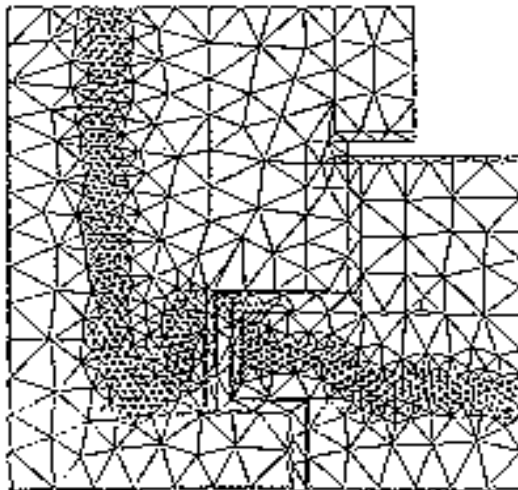


Fig. 3.16 Adaptive remeshing in phase change region [15].

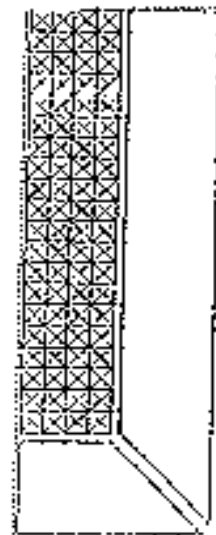


Fig. 3.17 Discretization of casting and mold [5].

The casting domain is divided into linear finite elements (triangle) whereas on the boundary of a mold domain boundary elements are distinguished (Fig 3.17). In comparison with FEM, for the same accuracy it needs considerably fewer internal cells and fewer boundary elements and can utilize a large time step. It has been found that computed results using the technique of FEM + BEM has sufficient accuracy [5].

3.4 Summary of Literature Review

Foundries try to eliminate all possible defects in the casting at early stage. Simulation technique simulates the casting process mathematically and optimises mold designs without test castings. However simulation programs run on expensive computer system. Computational time, accuracy and cost are three major factors to select a method for simulation.

Computational time Geometry driven methods give quick estimates of the possible defects under a particular set of process parameters. Where as computational time required for heat transfer approach is high due to large number of parameters and rigorous mathematics.

Accuracy Accuracy of the simulation technique largely depends upon the availability of data. Simulation technique requires knowledge of the thermal diffusivity, density and other thermo physical properties of all the components (metal, mold, chills, feeding aids). Many of these parameters are often unknown or difficult to determine. So there is difference in predicted and actual results (defects).

Cost The mathematics encountered in the use of classical heat transfer applied to three dimensional solidification is rigorous. So the need of expensive computer system for computation increases the cost of heat transfer approach. Geometry driven methods are less expensive due to simpler mathematics. While selecting a method one has to consider time, cost, and accuracy. G.Upadhya and A.J.Paul explained the effectiveness of geometry based approaches for solving casting design by arriving at approximate solution [17]. Subsequently a heat transfer approach is then applied. One of the advantage of using this methodology is that there is no need to create different inputs for geometry based and the comprehensive heat transfer calculation. The same set of part and process data can be used for both the calculations.

CHAPTER 4

SOLIDIFICATION SIMULATION SOFTWARE

4.1 Introduction

This chapter briefly describes the stepwise procedure for doing simulations with three software packages made available for the project:

- NovaSolid

NovaCast AB, Ronneby, Sweden has marketed this software and an education version is available in the Casting Simulation Laboratory (Mechanical Engineering Department of IIT Bombay).

- MAGMAsoft

The software has been developed by MAGMA GmbH, Kackertstra 11, D-52072 Aachen, Germany.

- PAMCAST/SIMULOR

ALUMINIUM PECHINEY, Casting Alloy Division, developed this software in conjunction with ESI group. The MAGMAsoft and PAMCAST/SIMULOR were made available at Centro Ricerche Fiat Turin, Italy.

4.2 NovaSolid

This software comprises of five modules:

- Build Geometry
- Initial Conditions
- Simulation
- Browse Results
- Material Database

4.2.1 Build Geometry

Following are the few functions of this module:

File conversion: In Build Geometry CAD files are imported and converted to the internal NovaSolid format *.FLT. The formats that can be converted are STL as both ascii and

binary, DXF in 3D form for example AutoCAD, CAT a format, which enables direct import from CATIA, and FLT files created in earlier versions.

Rotation: The imported solid can be rotated for proper orientation of casting.

Unit Conversion: The user has the possibility to change between different units, for example between inch and millimeter.

Figure 4.1 shows the picture of imported file in Build Geometry.

4.2.2 Initial Conditions

In Initial Conditions module, all the casting parameters are set and the final preparation for the simulation is made. The few functions of this module include:

Meshing: Meshing can be done by selection of cube size or total number of cubes.

Set Materials: The materials for casting and mold can be selected using this function.

Set Thermocouple: By placing the thermocouple in different parts of the casting, the temperature changes, its first derivative and the change in liquid fraction can be monitored as the simulation progresses.

Coatings: Coatings can be added to any surfaces.

Boundary Conditions: Different boundary conditions are available for choice such as Constant temperature, Normal, Heat radiation. Figure 4.2 shows the picture of Initial Conditions.

4.2.3 Simulation

Solidification calculations are made in the simulation module. Before the simulation, user has to set parameters like end simulation criteria, step of autowriting simulation file, maximum calculation step between two calculations.

Simulation can be viewed in different screen pictures called fields in the NovaSolid program. These are:

Temperature: This feature allows the user to see the temperature in the objects. The temperature can be checked in cross-section in every point.

3D shrinkage: Shrinkage is predicted with this function.

2D shrinkage: Shrinkage defects are shown from three directions giving a good position of the defects.

Figure 4.3 shows Mesh field, Temperature field, Liquid fraction field and Shrinkage at the selected section.

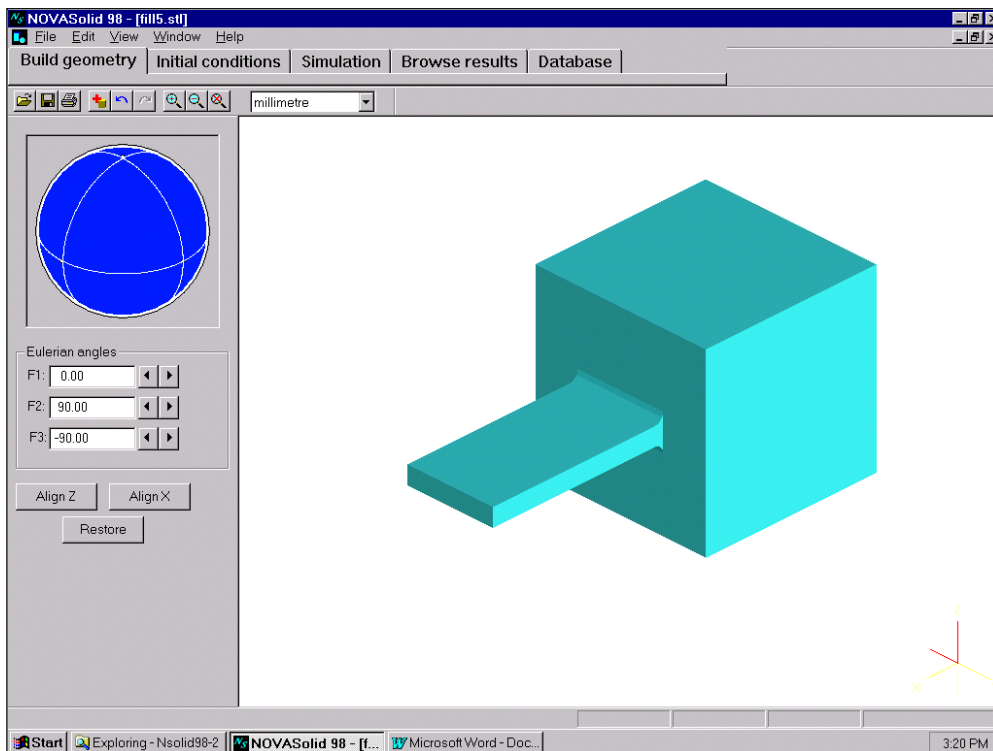


Fig. 4.1 Picture of imported file in Build Geometry module.

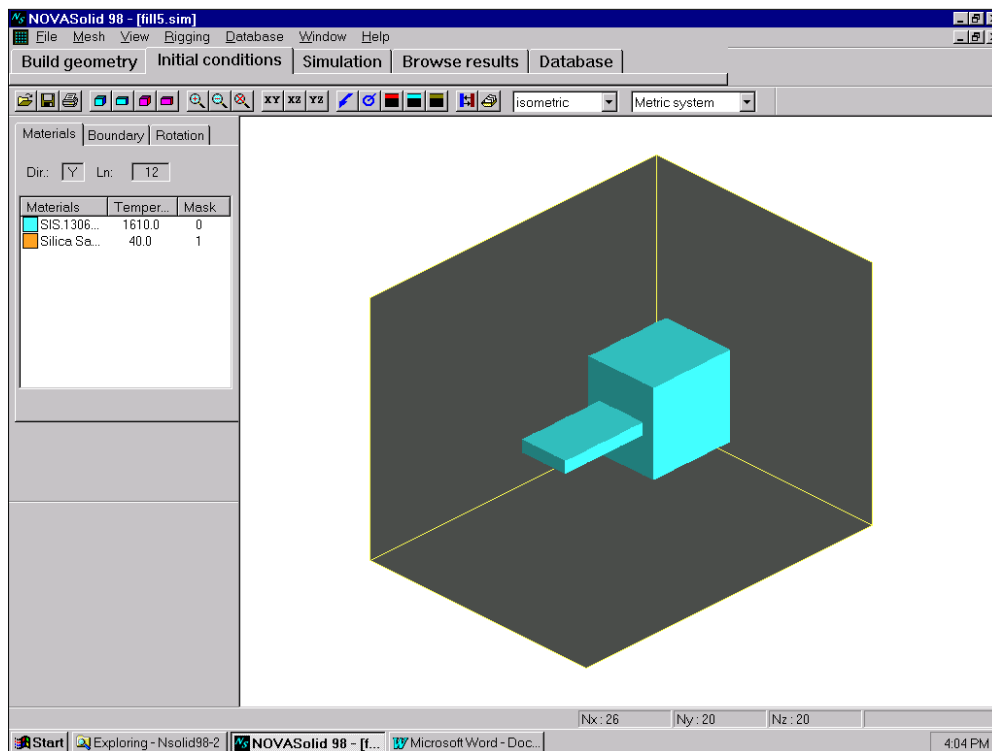


Fig. 4.2 Picture of Initial Condition module.

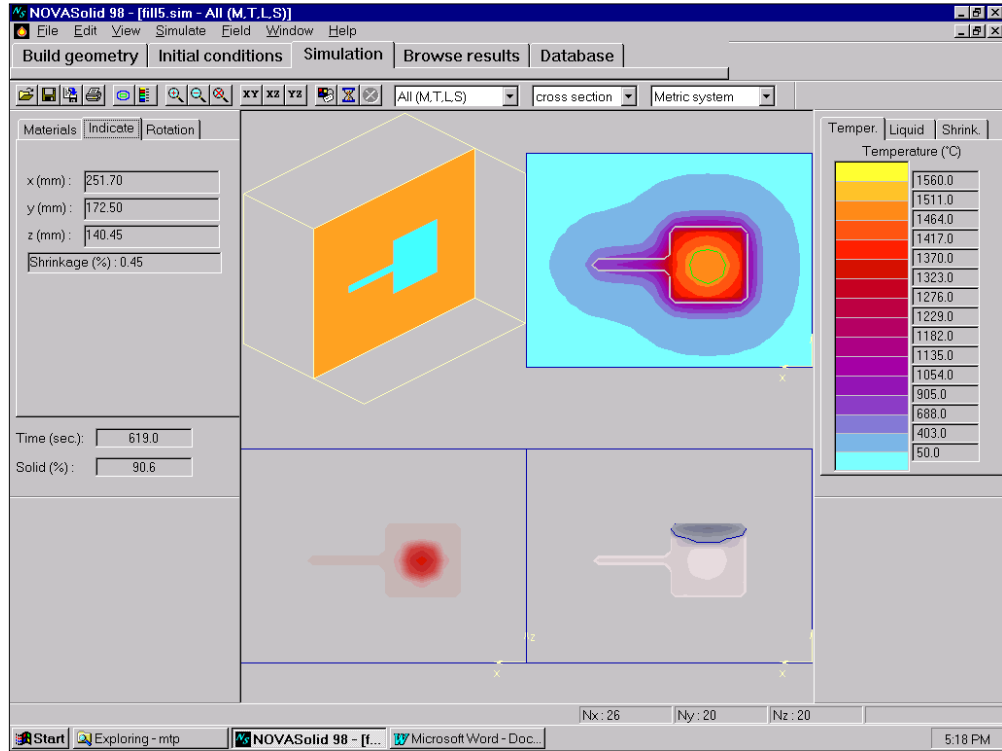


Fig. 4.3 Mesh, Temperature, Liquid fraction and Shrinkage Field.

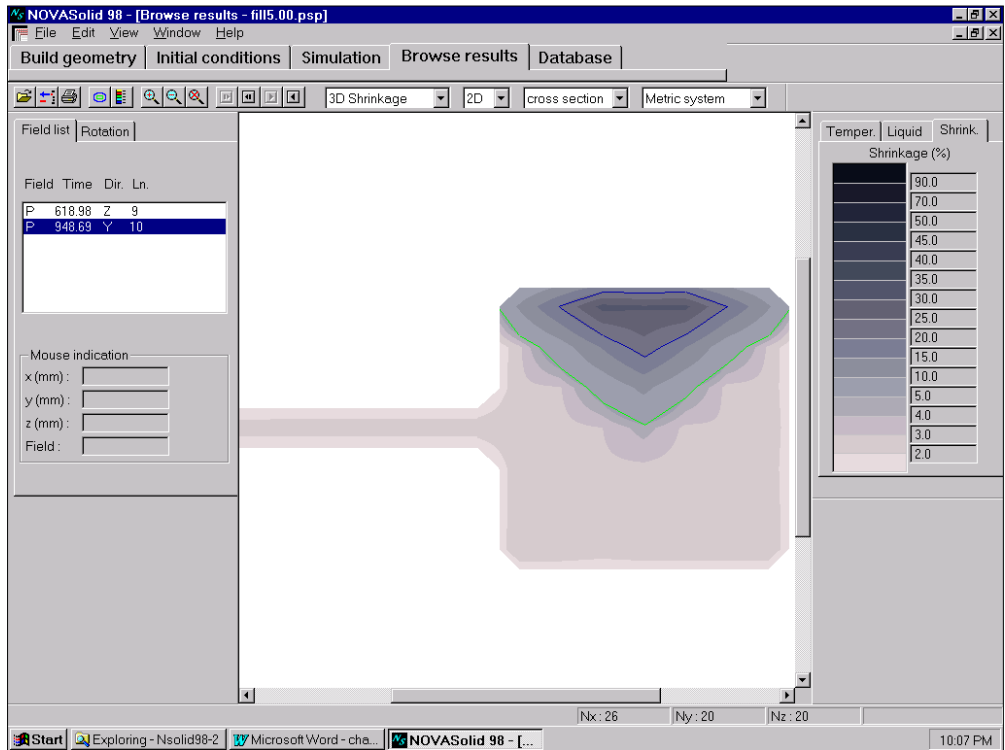


Fig. 4.4 Shrinkage result saved in Browse Result module.

4.2.4 Browse results

In the Browse results module the autosaved and the manually saved simulation results can be viewed and evaluated. The result can be viewed in 2D or 3D, cross section or isometric. The following functions are available in the Browse results module:

1. Rotation of the casting box.
2. Measurement scale.
3. Indicate function (getting information from the picture).
4. Play function.

Figure 4.4 shows the shrinkage result at slide 10 in Y direction.

4.2.5 Database

The database is used to specify the materials for simulations. The most common types of cast alloys in the foundry are available in the database. The material specification is in the Swedish alloy standard. Figure 4.5 shows the data for Grey iron in Database module. The different materials available by default include: Steels (Carbon steel, Alloy steel, High alloy steel), Grey iron, Aluminum base alloys, Copper base alloy and Mould materials.

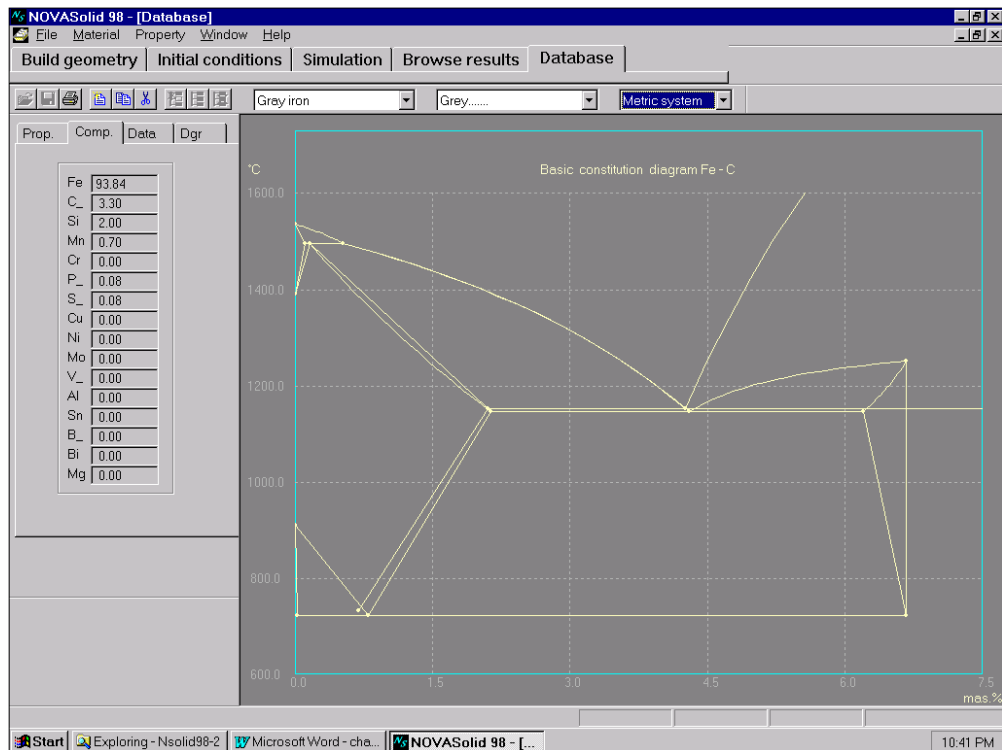


Fig. 4.5 Constitution diagram for Grey iron in Database module.

The database of a typical material consists of different data such as: Heat conduction, Specific heat, Density, C.L.E (Coefficient of linear expansion) and Constitution diagram. In addition the user can create a new material, can change existing material or can delete the material from database

4.3 MAGMAsoft

This software comprises of following seven modules:

- Project management module
- Preprocessor module (MAGMApre)
- Mesh generator module (MAGMAmesh)
- Mold filling module (MAGMAfill)
- Solidification module (MAGMASolid)
- Postprocessor module (MAGMApost)
- Database management module (MAGMAdata)

4.3.1 Project management module

This is the first module to start the simulations in MAGMAsoft. The operations that can be performed in this module include:

- Creating a new project
- Opening an existing project
- Create a new version of a project
- Delete version or delete project

The Fig. 4.6 shows the screen print of MAGMAsoft to open project named trial with Version_0.

4.3.2 Preprocessor module (MAGMApre)

The Fig. 4.7 shows the picture of geometry modeling in MAGMApre. The important operations performed in this module include::Modeling of the geometry, Import of CAD data, Manipulation of the geometry, Control point definition ,Material group assignment.

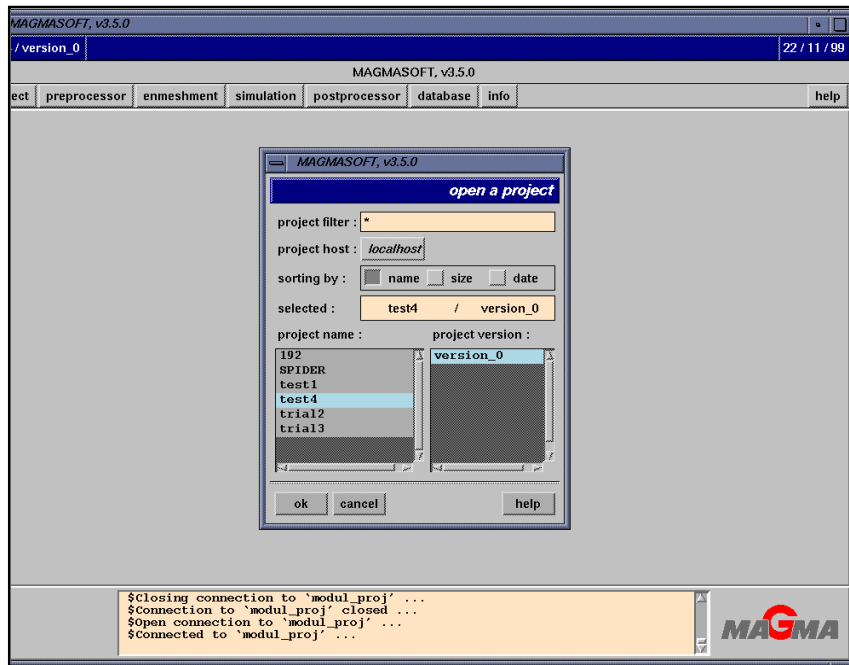


Fig. 4.6 Picture of Project module of MAGMAsoft to open a project.

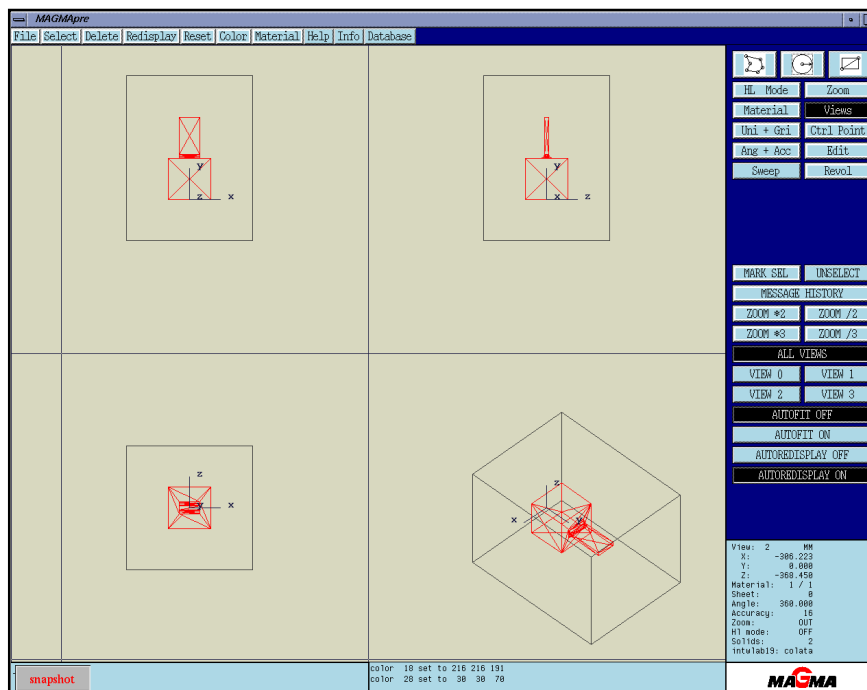


Fig. 4.7 Picture of MAGMApre for modeling a geometry.

4.3.3 Mesh generator module (MAGMAmesh)

After modeling the geometry in MAGMApre, the geometry is needed to be divide into the small control volumes by the process known as mesh generation. MAGMASoft mainly does the work of mesh generation but user has control over the significant variables of the enmeshment. The parameters that have to be defined in mesh generator are Method (Standard/Advanced), Accuracy (number of times each element should be further subdivided), Wall thickness (surface details smaller than wall thickness not captured in the mesh generation), Element size (minimum possible size of the element), Smoothing (maximum allowable value for the ratio of lengths of neighboring elements), and Aspect Ratio (Maximum allowable length to width ratio of a mesh element). Fig. 4.8 shows the picture of mesh generator module to define the different meshing parameters.

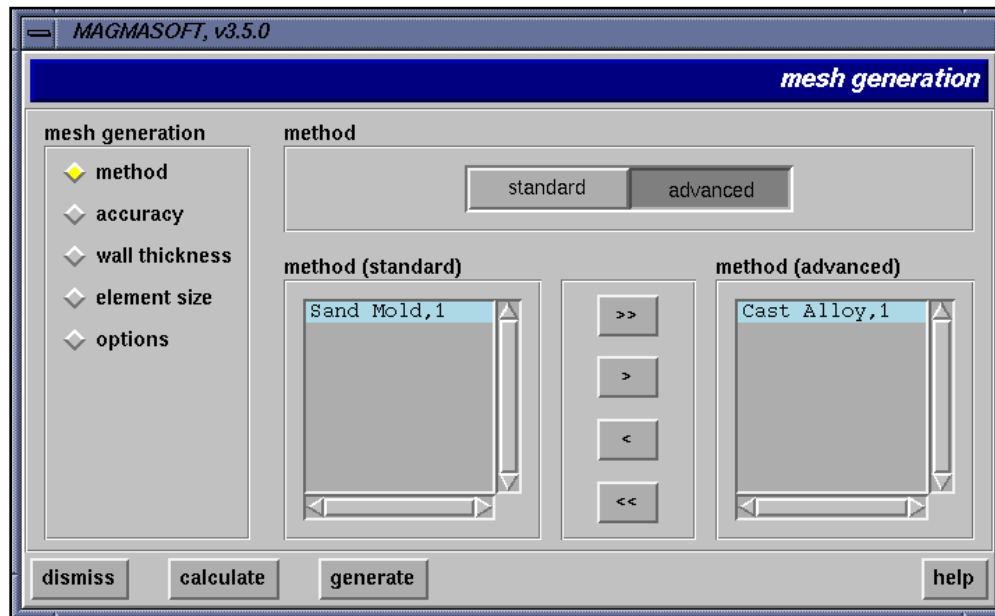


Fig. 4.8 Picture of Mesh generation module.

4.3.4 Mold filling module (MAGMAfill)

After modeling the geometry of casting and executing the meshing operation, some process parameters are needed to set for starting the simulations. There are some common definitions for both filling and solidification simulations like material definitions, heat transfer definitions between the individual domains. After the common definitions filling parameters has to be defined which includes filling time/pouring rate,

filling direction etc. Fig. 4.9 shows the picture of filling definition where the choice of solver and definition of filling parameters can be made.

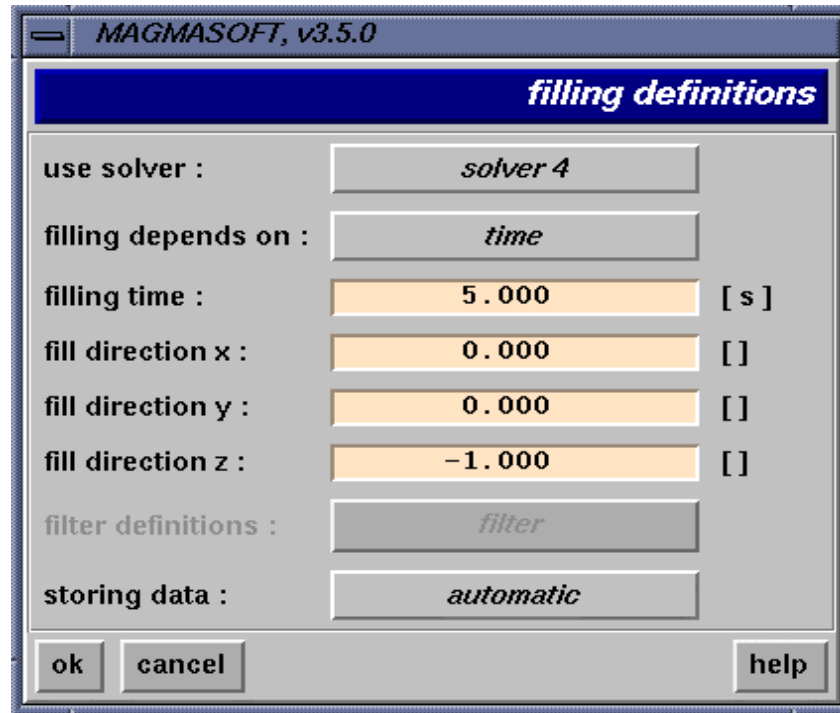


Fig. 4.9 Picture showing filling definition for MAGMAfill module.

4.3.5 Solidification module (MAGMASolid)

The casting can be simulated as only for solidification or for both filling and solidification. For solidification simulation user has to enter the solidification parameters like solver choice, stop simulation temperature or time, feeding effectivity and criteria temperatures. Figure 4.10 is the picture for solidification definition in MAGMASoft.

4.3.6 Postprocessor module (MAGMApost)

The results of the simulations can be viewed in MAGMApost. The different options are available for the better interpretation of filling/solidification simulation results. The quality of mesh can also be viewed in MAGMApost. The types of results include cooling curves, filling tracer, porosity, temperature gradient distribution, and Niyama criteria. The options for viewing include clipping, rotation, color scale viewpoint, and zoom. The Fig. 4.11 shows the picture of MAGMApost module

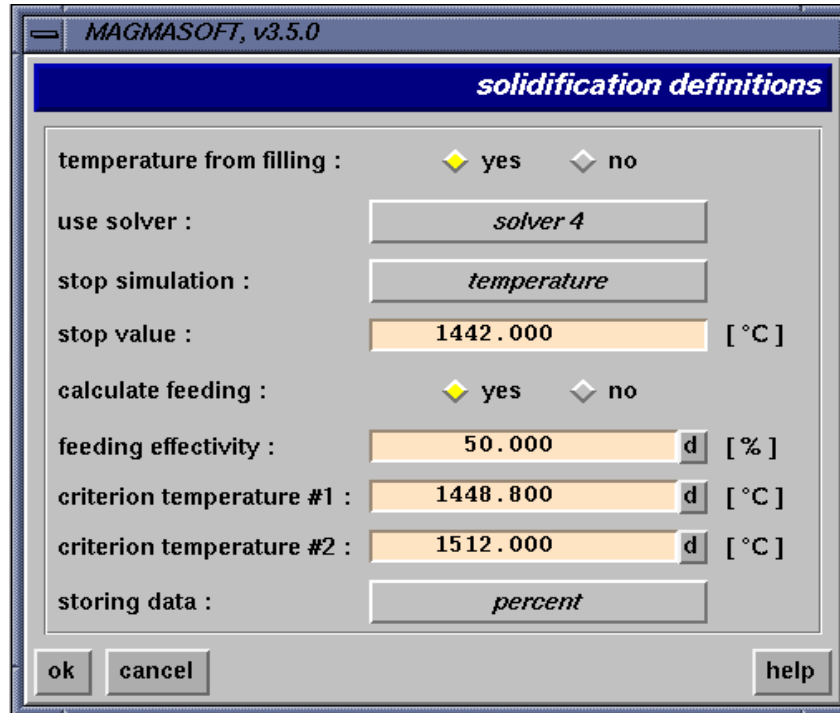


Fig. 4.10 Picture showing solidification definition for MAGMASolid module.

2.3.6 Database management module (MAGMAdata)

MAGMASoft provides the data for cast alloy, molding material, core, insulation, coatings and chill. Typical material data includes liquidus temperature, solidus temperature, latent heat and properties like thermal conductivity, density, specific heat capacity, fraction solid, viscosity, flow properties and thermal expansion coefficient. In MAGMAdata it is possible to create a new data or modify the current data or delete the data from database. MAGMAdata also stores the information about the internal and external heat transfer coefficient as constant or temperature or time dependent. Figure 4.12 shows the picture of MAGMAdata.

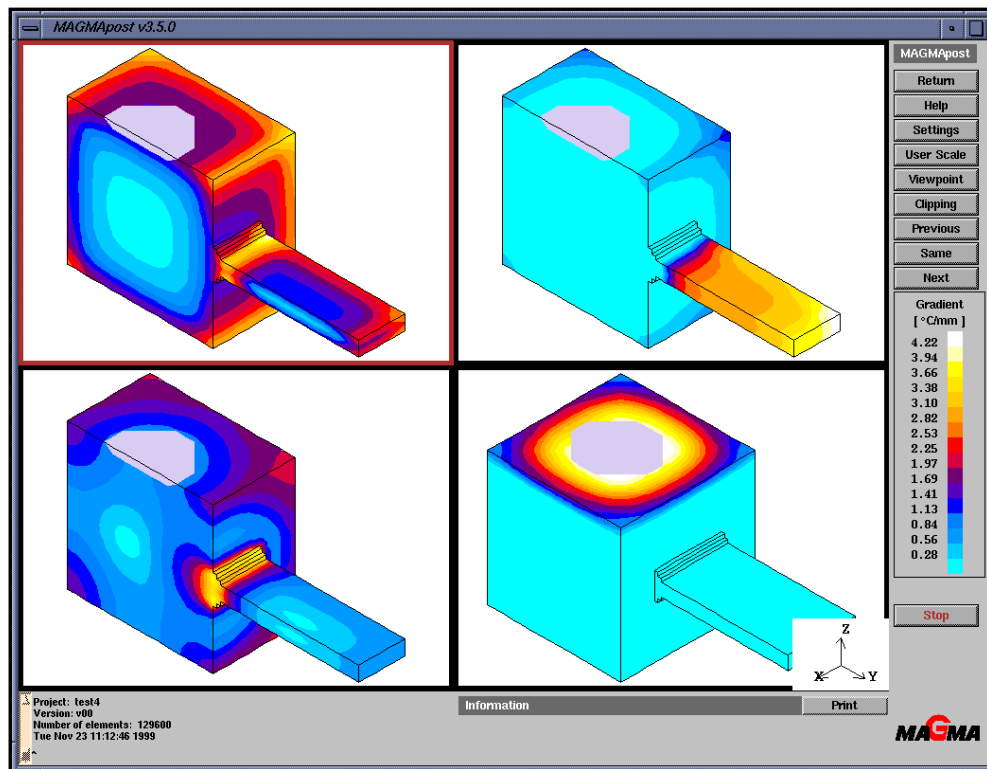


Fig. 4.11 Picture of MAGMApost module.

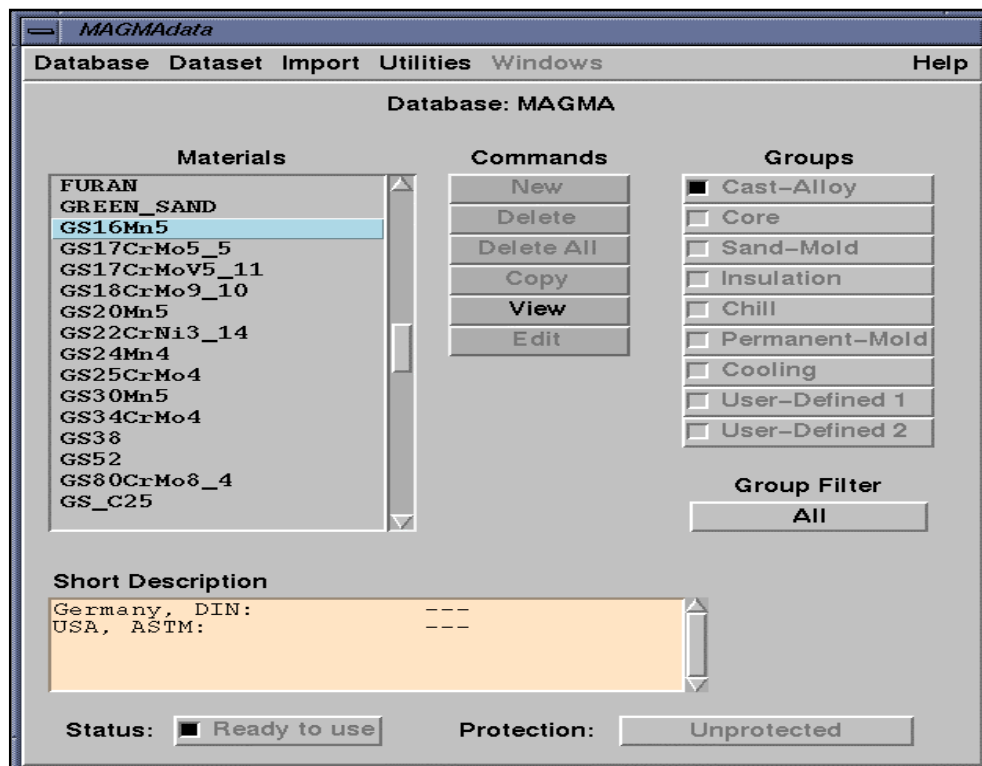


Fig. 4.12 Picture of MAGMAdata module.

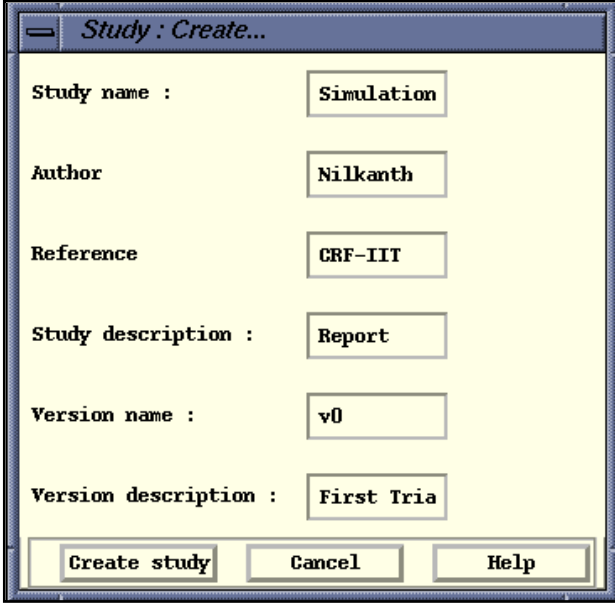
4.4 PAMCAST/SIMULOR

This software has following seven modules.

- Study
- Surface Model
- Volume Model
- Data Assignment
- Calculations
- Results
- Database

4.4.1 Study

Creation of the Study is the first step to start with SIMULOR. The Fig. 4.13 shows the steps to create a new study. The study consists of one or more versions of the calculations. The other operations that can be performed in Study menu include Open (Opens an existing project), Save (Saves the changes made in active study), Save version (To save current version and to create a new version of the current study), Duplicate (Duplicate a study) and Deletes (To delete a version of a study or to delete a study with all versions).



Study name :	Simulation
Author	Nilkanth
Reference	GRF-IIT
Study description :	Report
Version name :	v0
Version description :	First Tria

Buttons: Create study, Cancel, Help

Fig. 4.13 The picture of Study menu to create a new study.

4.4.2 Surface Model

This module is used to import a single geometric model or several geometric models from the CAD program. Importing CAD mesh convert the surface mesh into a completely triangular surface mesh. The Fig. 4.14 shows the picture of imported CAD mesh into SIMULOR.

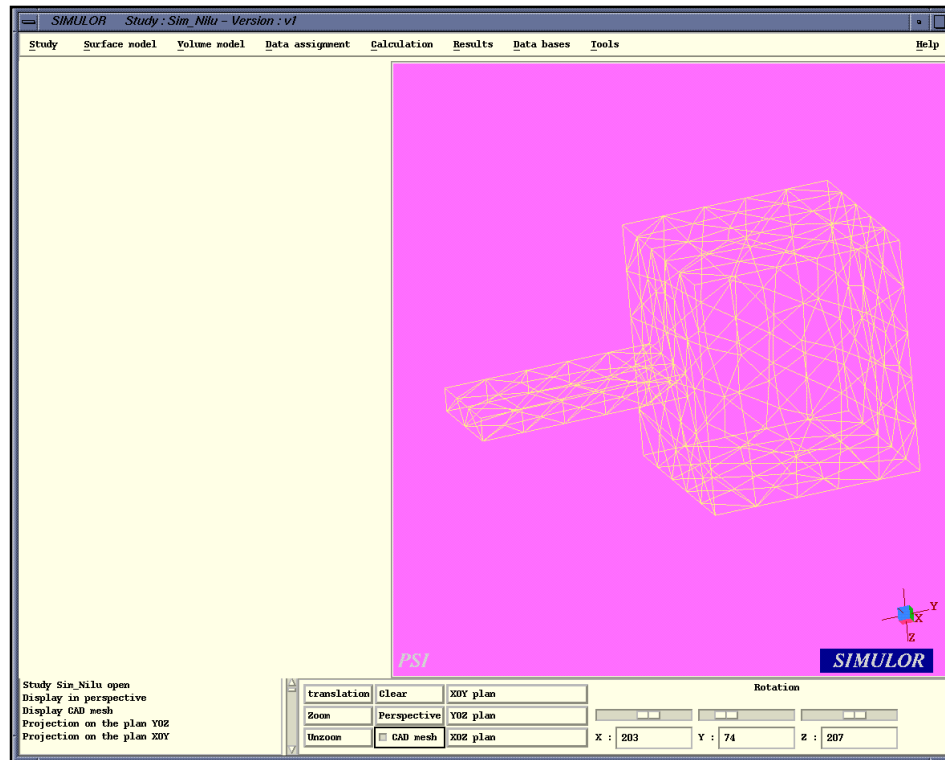


Fig. 4.14 Import of CAD mesh in SIMULOR.

4.4.3 Volume Model

The operations performed in this module include Rename Regions (For renaming of volume regions), Delete Regions (For deletion of volume regions), Material Assignment (To assign a material or to modify the assignment of a material to a volume region), Mesh generation (To generate the mesh), and Grid (To check quality of the grid and to modify the existing grid on each axis). The Fig. 4.15 Shows the grid information and picture shows the grid on X and Y axis.

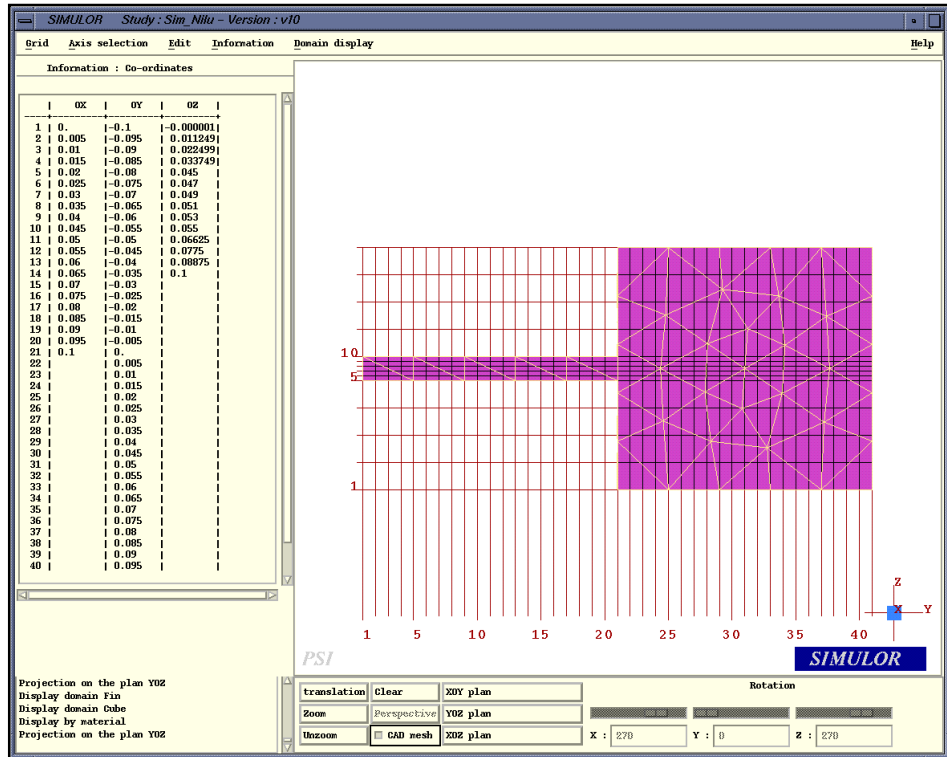


Fig. 4.15 Grid information in Volume Model.

4.4.4 Data Assignment

The values for the parameters and boundary conditions are defined in this module. The list of parameters include die coating parameters, air gap parameters, hydraulic conditions for filling, thermal conditions for filling and solidification, physical parameters for solidification and details about the implicit mold. Fig. 4.16 shows the physical parameter assignment for solidification.

The screenshot shows the "Solidification..." dialog box. It contains the following text and input fields:

For Niyama criteria calculation (Cooling rate):

- Temperature difference from solidus(C)

For shrinkage calculation:

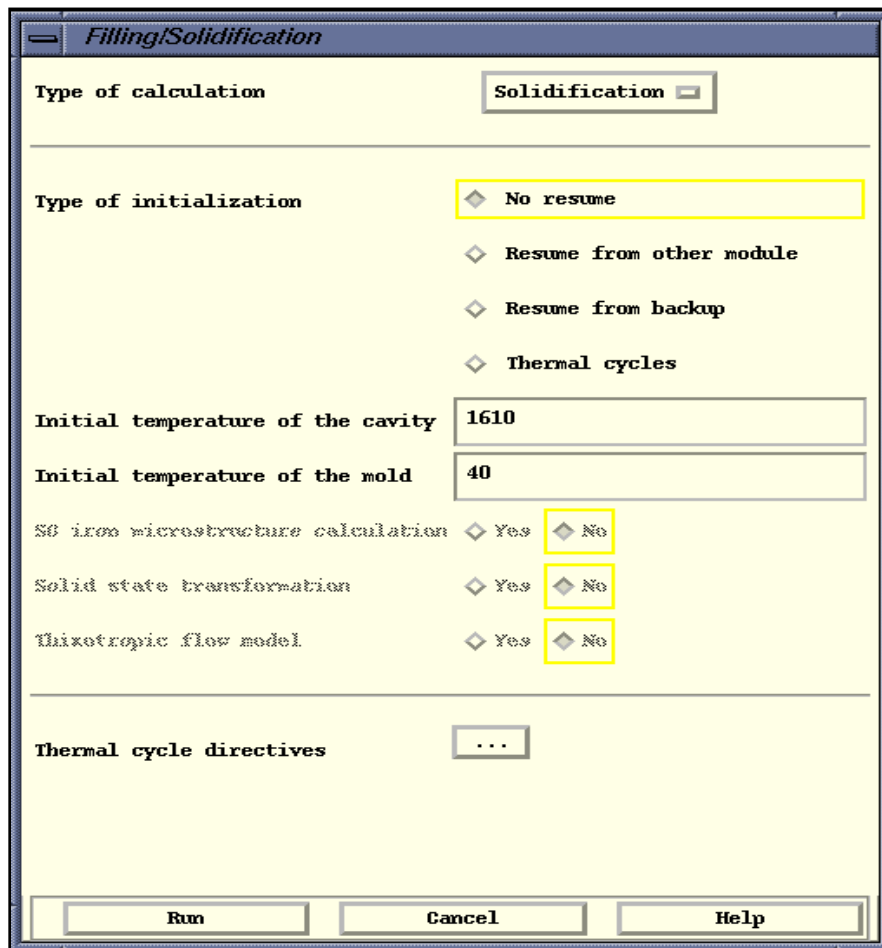
- End of mass feeding solid fraction
- Critical solid fraction
- SG iron microstructure

At the bottom, there are three buttons: "Ok", "Cancel", and "Help".

Fig. 4.16 Definition of physical parameters for solidification.

4.4.5 Calculations

This menu is used to define the parameters for calculations, to start the calculations and to stop the calculations. The various calculations that can be performed include only filling, only solidification, filling and solidification and defect calculations. The Fig. 4.17 shows the definition of solidification calculation with the cavity temperature of 1610 °C and mold temperature of 40 °C.



The screenshot shows a dialog box titled "Filling/Solidification". The "Type of calculation" is set to "Solidification". Under "Type of initialization", "No resume" is selected. The "Initial temperature of the cavity" is 1610 and the "Initial temperature of the mold" is 40. For "SG iron microstructure calculation", "Solid state transformation", and "Anisotropic flow model", the "No" radio button is selected. There is a "Thermal cycle directives" button with an ellipsis. At the bottom are "Run", "Cancel", and "Help" buttons.

Parameter	Value / Option
Type of calculation	Solidification
Type of initialization	No resume
Initial temperature of the cavity	1610
Initial temperature of the mold	40
SG iron microstructure calculation	No
Solid state transformation	No
Anisotropic flow model	No
Thermal cycle directives	...

Fig. 4.17 Parameters to run the solidification calculation.

4.4.6 Results

The different options in this module are Mesh (For CAD visualization and meshing display, Filling (To see the results of filling), Solidification (To see the temperature history in the casting or to see the liquid fraction), Solidification synopsis (To see the liquidus isochron, Local cooling rate, etc.), Defects (To see the Shrinkage

defect, Dendrite Arm Spacing, Niyama Criteria and Solidification rate) and Graphs (To see the temperature verses time or to see the % liquid verses time at the specific points). Figure 4.18 shows the predicted Shrinkage result in a casting section.

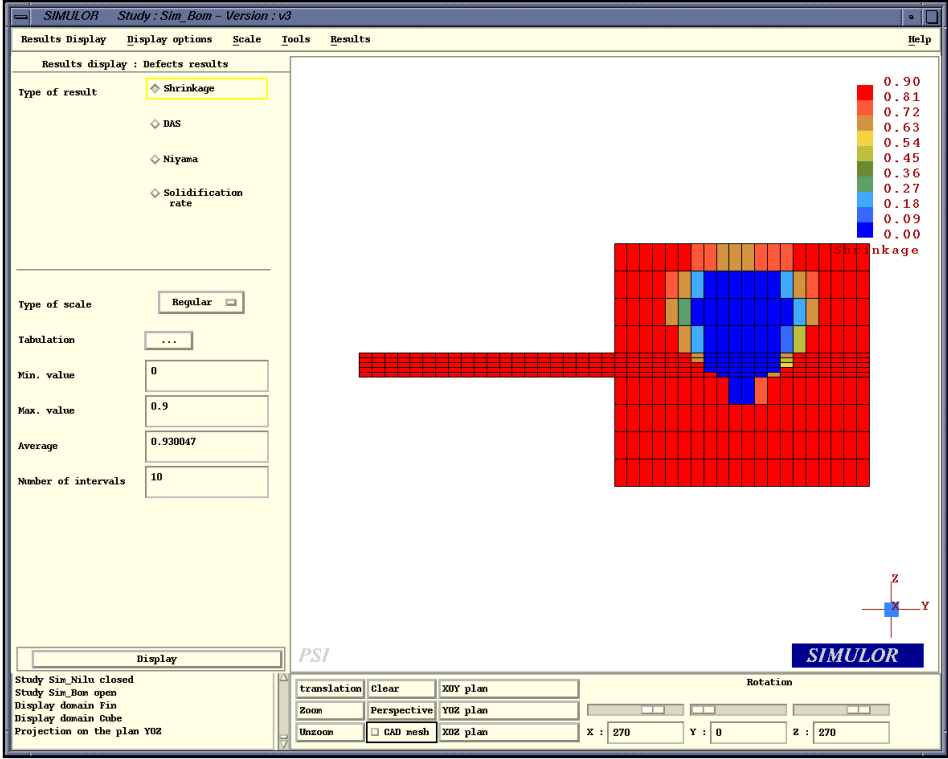


Fig. 4.18 Predicted shrinkage result in a casting section.

4.4.7 Databases

The database consists of Alloy database, Mold database, Die coatings database and Air gap database. A new data can be created or the existing one can be manipulated. The manipulation commands are Create, Delete, Duplicate and Modify.

4.5 Case study for comparison

For general comparison a simulation with NovaSolid, MAGMASoft and SIMULOR is carried using same component. The Fig. 4.19 shows the STL picture of the model used for the simulations. Table 4.1 gives the details about the process parameters, material parameters, simulation parameters and results of simulations carried with each software to do the general comparison of software.

Table 4.1: Comparison of software package for the case study.

	NovaSolid	MAGMAsoft	SIMULOR
Input File	STL file	STL file	ICA file prepared in ANSA
Mold size	612*537*590 mm	612*537*590 mm	200 mm thick implicit mold
Cast metal	SIS 4244	Al Si 7Mg	Al Si 7Mg
Mold material	Green sand	Green sand	Green sand
Mesh elements in casting	30624	33076	36134
Pouring temperature	700 °C	700 °C	700 °C
Mold temperature	40 °C	40 °C	40 °C
Heat transfer coefficient	Air gap temperature 650 °C	2000 W/m ² K	2000 W/m ² K
Feeding effectivity	Not applicable	30 %	Not applicable
Critical solid fraction ratio	Not applicable	Not applicable	0.3
Mass feeding	Not applicable	Not applicable	0.1
Stop calculation criteria	100% Solidification	542 °C (solidus temperature)	542 °C (solidus temperature)
Calculation time	18 min	44 min	24 min
Total solidification time	513 s	189 s	209 s
Shrinkage	Fig. 4.20 (a)	Fig. 4.21 (a)	Fig. 4.22 (a)
Temperature distribution	Fig. 4.20 (b)	Fig. 4.21 (b)	Fig. 4.22 (b)

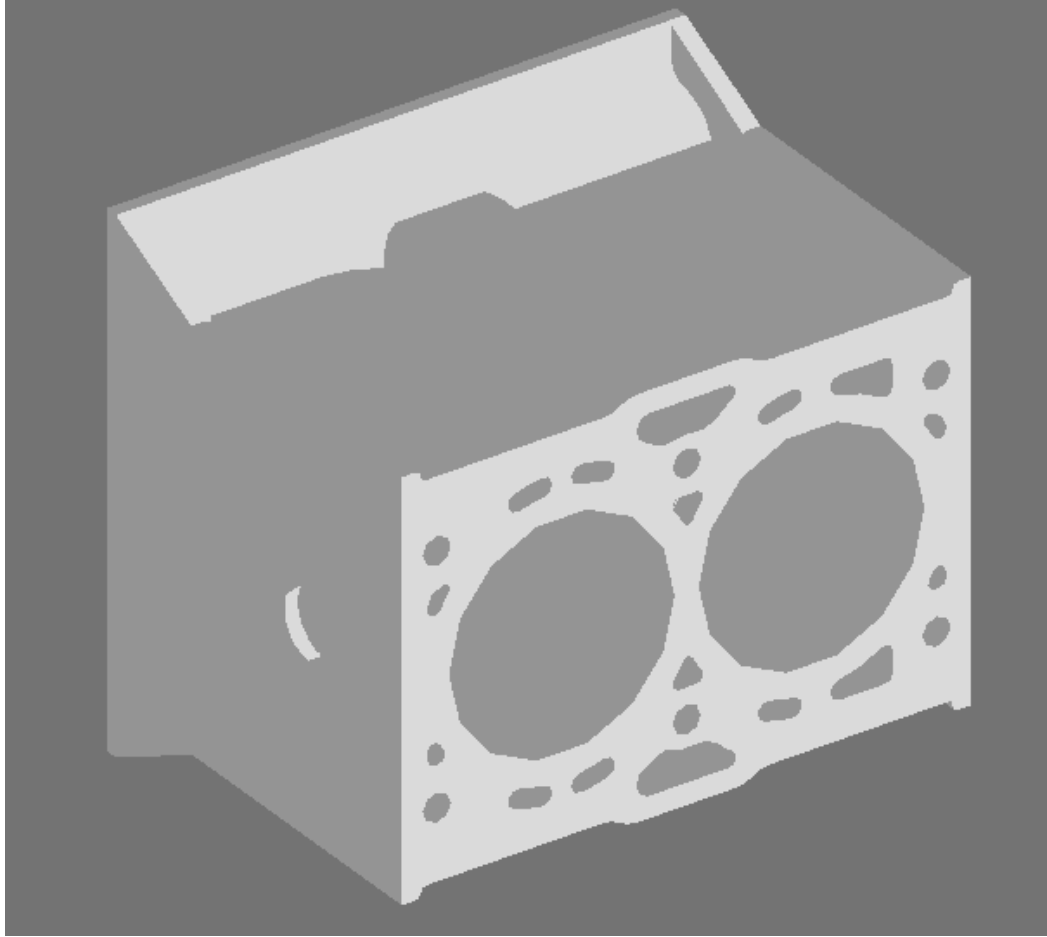
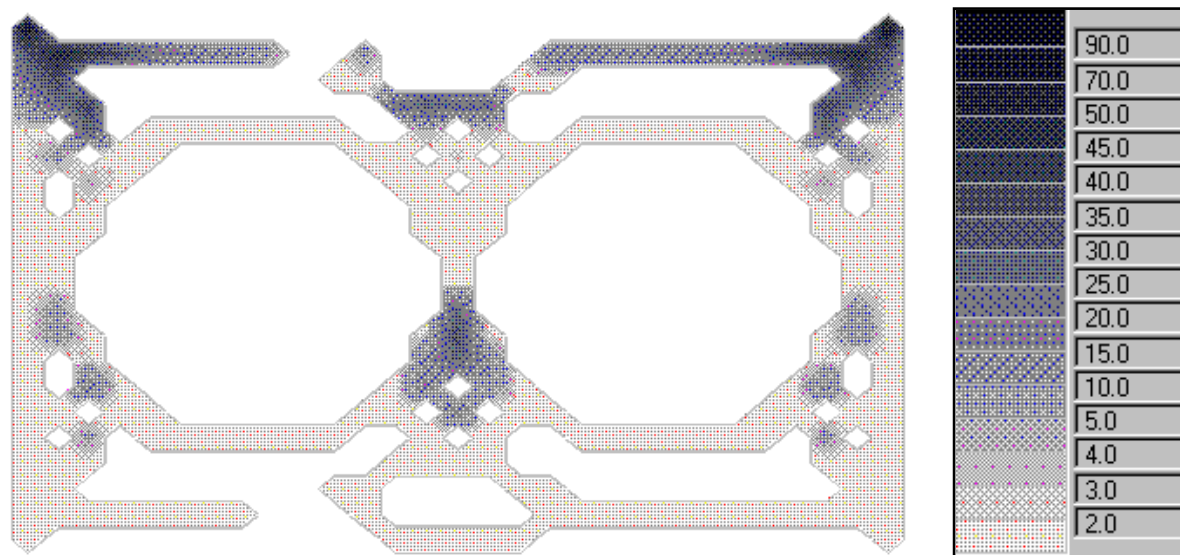
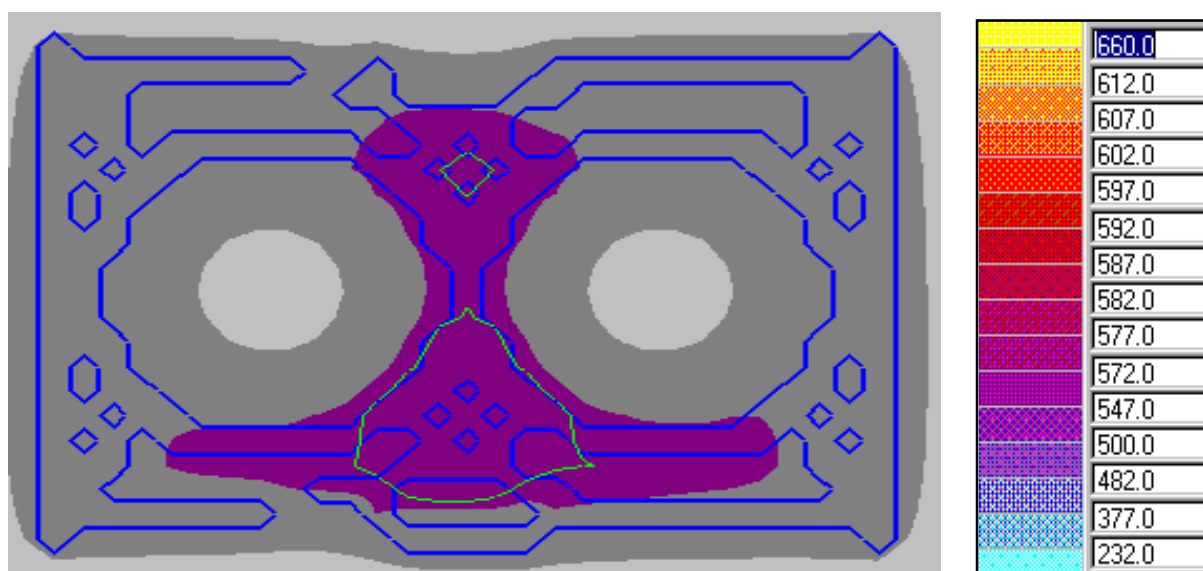


Fig. 4.19 Picture of STL geometry used for the simulations.

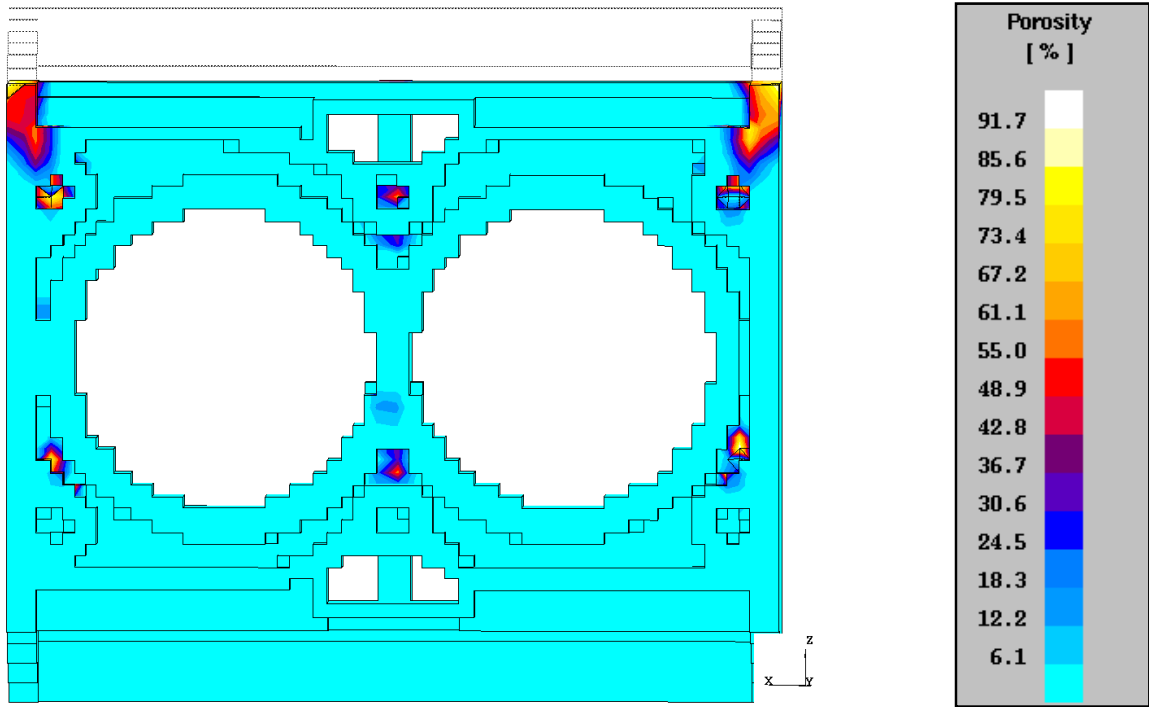


(a)

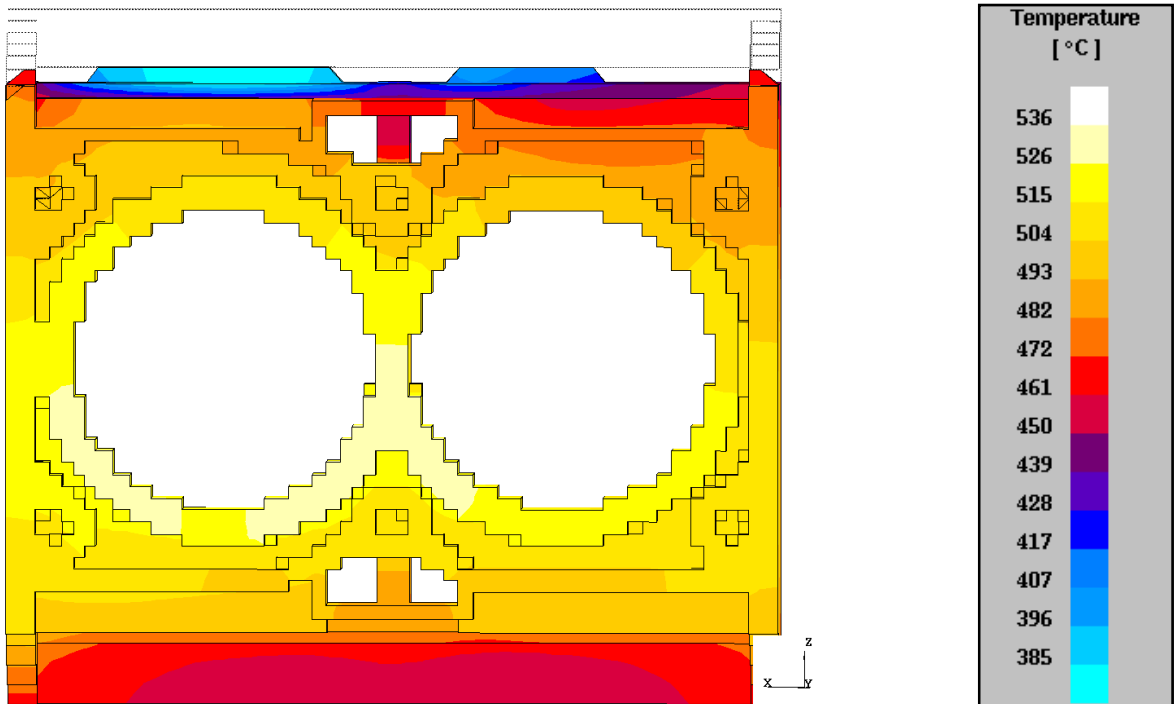


(b)

**Fig. 4.20 Predicted results with NovaSolid
(a) Shrinkage (b) Temperature distribution.**

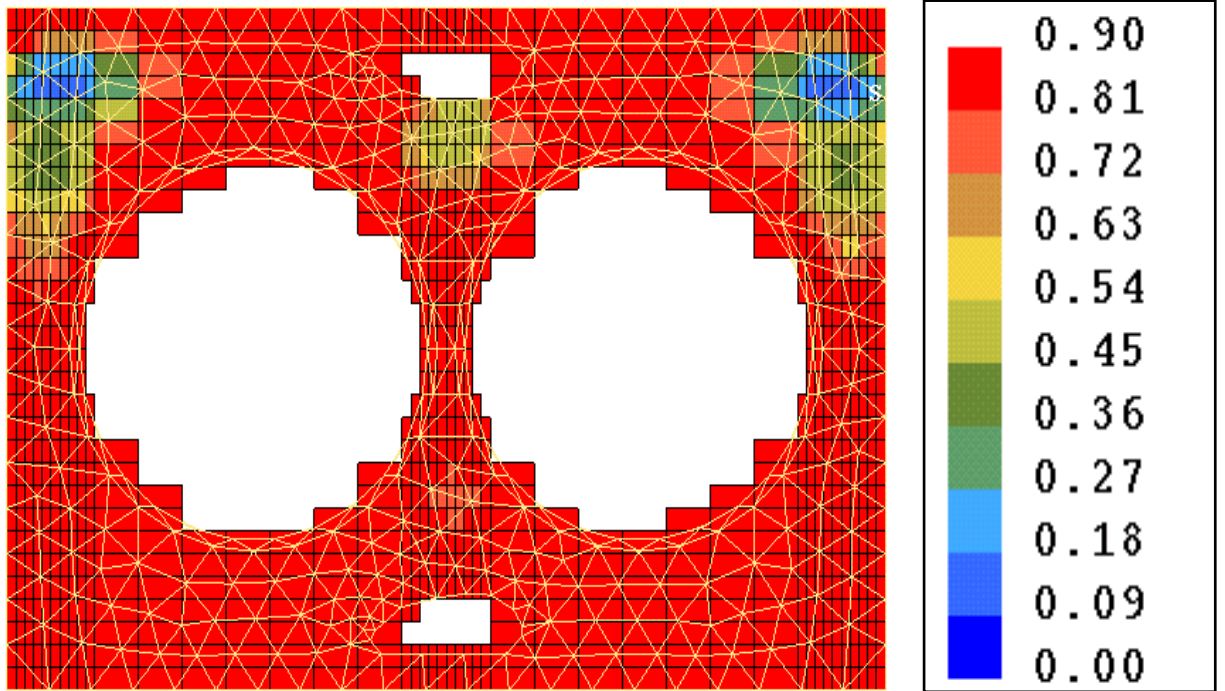


(a)

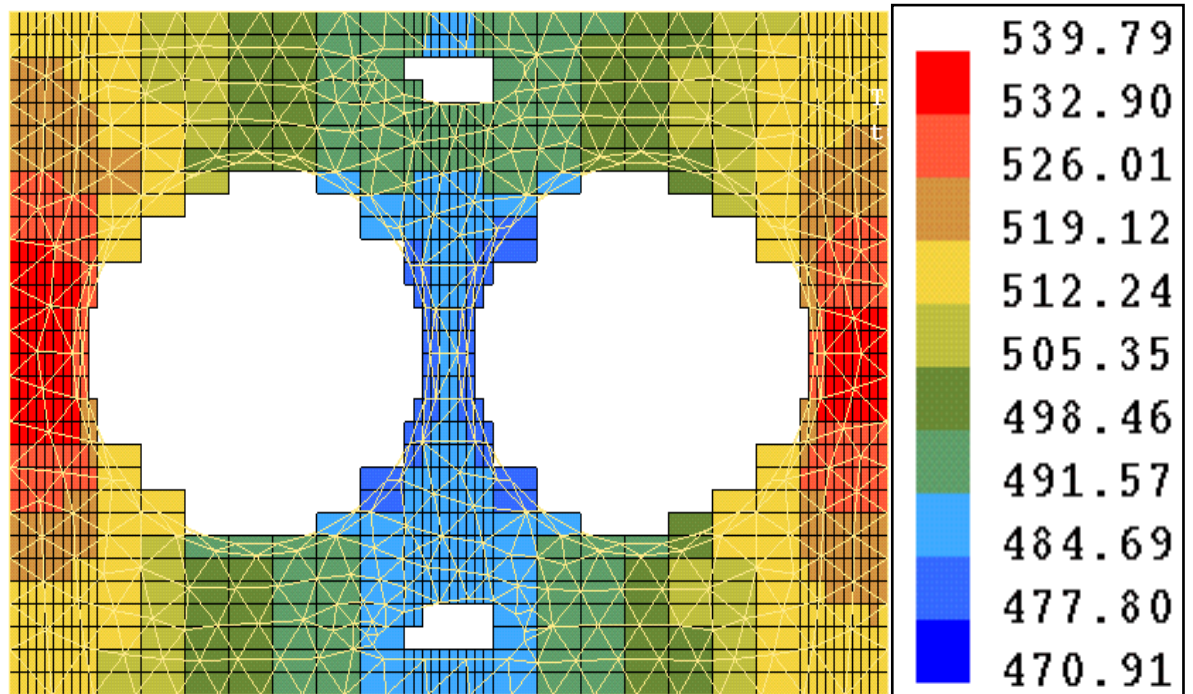


(b)

**Fig. 4.21 Predicted results with MAGMAsoft
(a) Shrinkage (b) Temperature distribution.**



(a)



(b)

**Fig. 4.22 Predicted results with SIMULOR
(a) Shrinkage (b) Temperature distribution.**

CHAPTER 5

SIMULATION EXPERIMENTS

5.1 Preliminary simulation experiments

The preliminary experiments were conducted with NovaSolid. The study has been made to find the different parameters for the further simulations with MAGMAsoft and SIMULOR.

5.1.1 Casting Shape and Dimensions

Figure 5.1 shows the shape of the casting designed for the simulation. The preliminary simulations were made so as to fix the dimensions. The solid models for this shape are prepared using ProEngineer solid modeler. Figure 5.2 shows the solid model for Fig. 5.1. The dimensions (length, width, thickness, fillet radius) of fin attached to cube can be varied to see the effect of dimensions on solidification simulation.

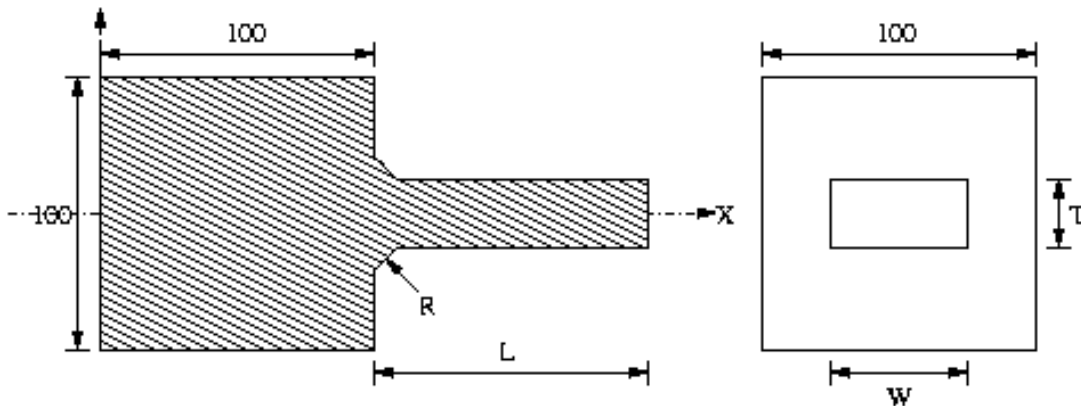


Fig. 5.1 Middle section of the casting used for simulation.

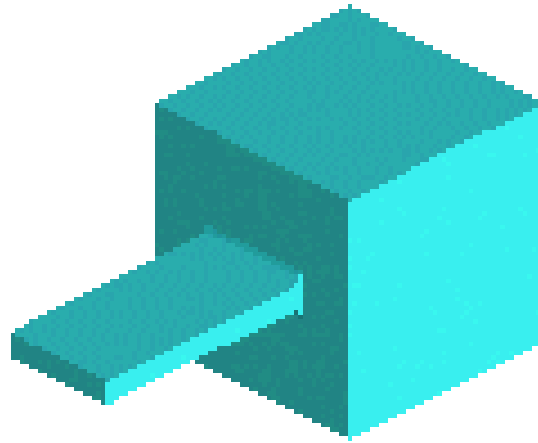


Fig. 5.2 Picture of solid model prepared in ProEngineer.

5.1.2 Design of experiments and results of simulation

The table 5.1 gives the design of experiment adopted for doing simulations with NovaSolid. The structure for sensitivity analysis is summarised in table 5.2. The graphs were plotted between the porosity values at the middle cross section and distance from the origin (extreme left of casting on the X-axis).

Table 5.1: Design of Experiments for NovaSolid.

Simulation No.	Material	Length mm	Width mm	Thickness mm	Fillet mm	Pouring Temperature °C
1	SIS 1306	100	50	10	0	1610
2	Ductile iron	100	50	10	0	1250
3	Grey iron	100	50	10	0	1315
4	SIS 4261	100	50	10	0	680
5	SIS 1306	125	50	10	0	1610
6	SIS 1306	150	50	10	0	1610
7	SIS 1306	100	50	10	5	1610
8	SIS 1306	100	50	10	10	1610
9	SIS 1306	100	10	10	0	1610
10	SIS 1306	100	50	10	0	1560
11	SIS 1306	100	50	10	0	1585
12	SIS 1306	100	50	10	0	1635
13	SIS 1306	100	50	10	0	1660

Table: 5.2 Sensitivity analysis for NovaSolid.

Simulation No.	Parameters	Results
1,2,3,4	Material	Fig. 5.3
1,5,6	Length	Fig. 5.4
1,7,8	Fillet	Fig. 5.5
1,9	Width	Fig. 5.6
1,10,11,12,13	Pouring temperature	Fig. 5.7

5.1.3 Discussions of results

(a) General conclusions from simulations

- (1) The maximum temperature at the end of solidification is at the center of the cube portion. This point ($X=50\text{mm}$) is the last point to solidify and acts as the feeding point.
- (2) The temperature along the fin length is highest at the junction of the fin and cube portion ($X=100\text{mm}$). The highest temperature gradient in most cases is found to be in fin area near to the cube portion ($X=110\text{mm}$).
- (3) The maximum porosity in all cases is found to be at center of the cube portion ($X=50\text{mm}$). At this point low temperature gradient is present. The temperature gradient at this point is lower but not the lowest. The local solidification time for all the cases is high at this point. Thus the porosity is not the function of temperature gradient alone but also it depends upon the local solidification time. These results are in good agreement with literature: low temperature gradients alone are not responsible for the formation of porosity. Lower values of the porosity at the both (fin and cube portion) end of the section show the feeding due to end effect. In most of the cases sudden rise in the porosity in the region $X=10\text{-}20\text{mm}$ (just after the beginning of cube portion) and $X=180\text{-}190\text{mm}$ (just before the end of the cube portion). Because of rapid solidification of walls at the end section, bridging across the section occurs which will hinders the flow of feeding metal from the feeder to the remote part of the casting.

(b) Effect of material

- (1) From Fig. 5.3 the porosity level for the casting shape is highest in case of SIS 1306, and porosity level is lower in case of Ductile and Grey iron. The porosity level for Aluminum alloy lies in between SIS 1306 and Ductile iron.

(2) The porosity distribution in fin portion is even in case of Grey iron, SIS 1306 and Ductile iron. In case of Aluminum alloy the porosity distribution is uneven. This is due to presence of very low temperature gradients in case of Aluminum alloy casting.

(3) The low level of porosity in Grey iron casting can be supported by the theory that the graphite flakes form in contact with the interdendritic liquid. The expansion (which occurs because, carbon takes up more volume in graphite form) that takes place acts directly on the liquid, forcing it up the interdendritic channels into any incipient pores, which would otherwise form in casting. This can be lead to conclusion that the tendency towards formation of pores is small in Grey iron casting.

(4) Proper care should be taken while designing the Aluminum alloy casting, as the porosities are unevenly distributed. Also the maximum value of porosity is with Aluminum alloy.

(5) Total solidification time is highest for Grey iron and lowest in case of Aluminum alloy. The difference in solidification time for SIS 1306, Aluminum alloy, and Ductile iron is not as much, though there is large difference in pouring temperatures. This explains the mushy freezing in Aluminum alloy and Ductile iron, and skin freezing in SIS 1306 (low carbon steel).

(c) Effect of length (L)

(1) From Fig. 5.4, it can be seen that, porosity level in fin portion is maximum for 150mm length of fin and minimum for 100mm fin length.

(2) Higher value of porosity at the center of cube portion for 100mm length compared to porosity values of 125 and 150mm lengths is due to prolonged solidification (Higher solidification time) at that point.

(d) Effect of fillet radius (R)

(1) Effect of higher temperature, lower temperature gradient and prolonged solidification time at the junction point with increase in fillet radius, increases the porosity. It can be observed from the Fig. 5.5.

(e) Effect of width (W)

(1) For the same conditions of castings with only change in width of fin section, the porosity is higher in case of 10mm wider casting than 50mm wider casting. The magnitudes of temperature gradients in fin area are higher for 10mm wider casting.

Absence of lateral feeding from sidewalls in 10mm wider plate due to rapid solidification from the side walls result into higher porosity values (Fig. 5.6).

(2) The solidification time is small in case of 50 mm wider section compared to 10mm wider casting. This is because of increase in surface area for heat transfer.

(f) Effect of pouring temperature

(1) From Fig. 5.7, in the middle portion of the fin portion (X=120 to 180mm) the porosity values are constant for all pouring temperature. The lowest porosity level is with pouring temperature of 1610 °C (100 °C superheat). The highest porosity level along this much of length is with pouring temperature of 1635 °C (125 °C superheat).

(2) The porosity is evenly distributed in fin portion (thin section) for all temperature but for cube portion (thick section) porosity distribution is near to even with only pouring temperature of 1585 °C, for all other pouring temperature the porosity distribution is uneven.

(3) At the junction of the cube and fin portions the porosity level is lowest for highest pouring temperature 1660 °C, where as for all other pouring temperatures the porosity value is same.

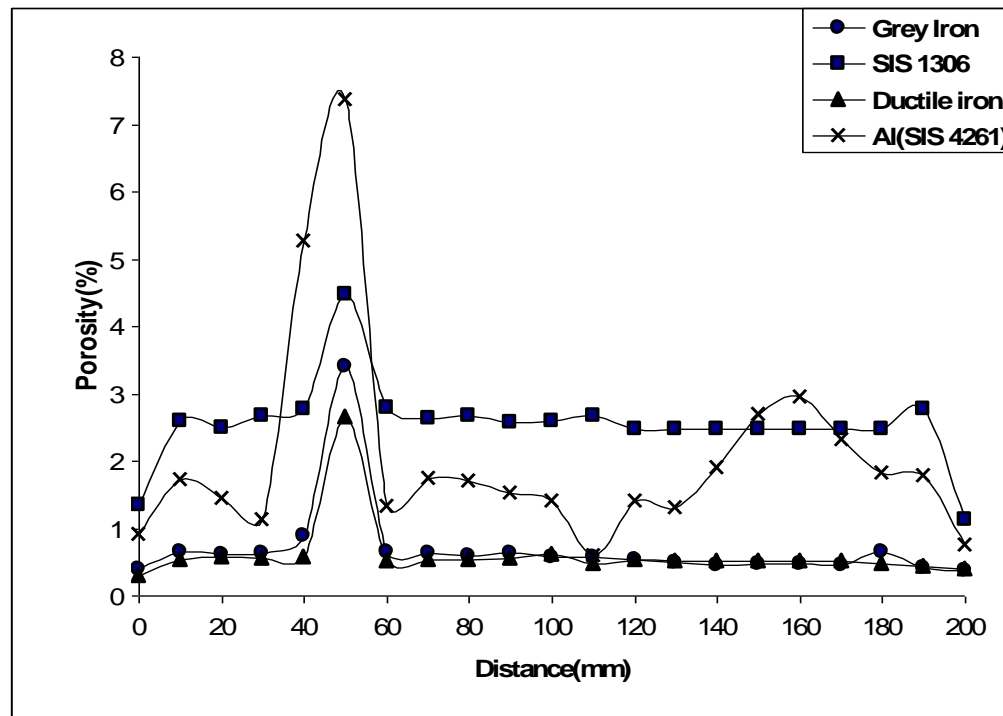


Fig. 5.3 Porosity values along X-axis for different materials.

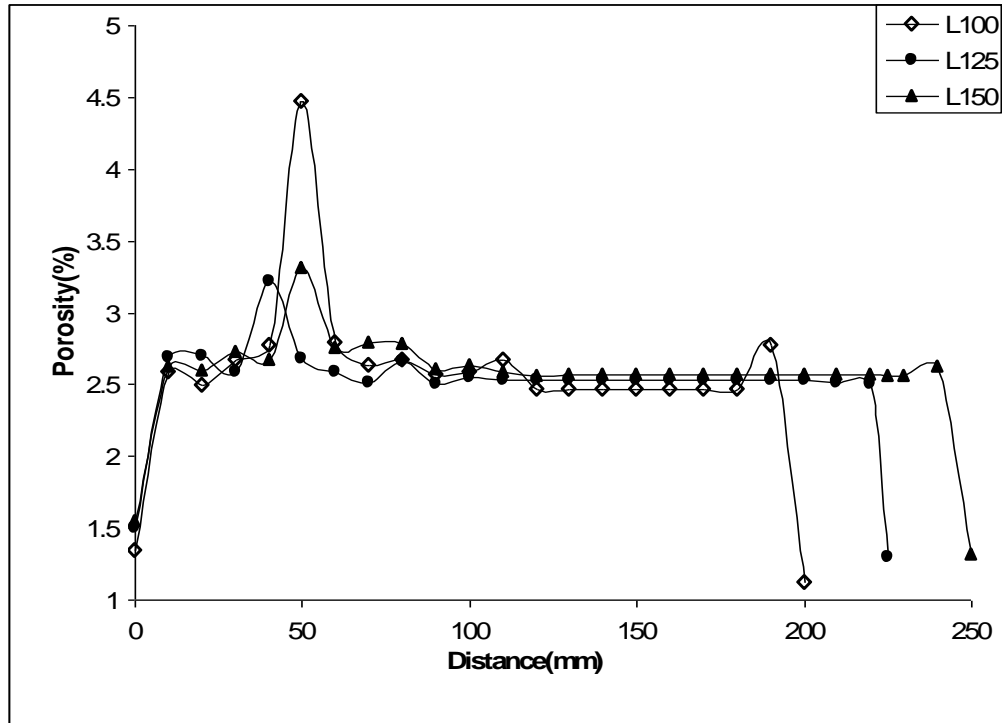


Fig. 5.4 Effect of length on porosity values along X-axis.

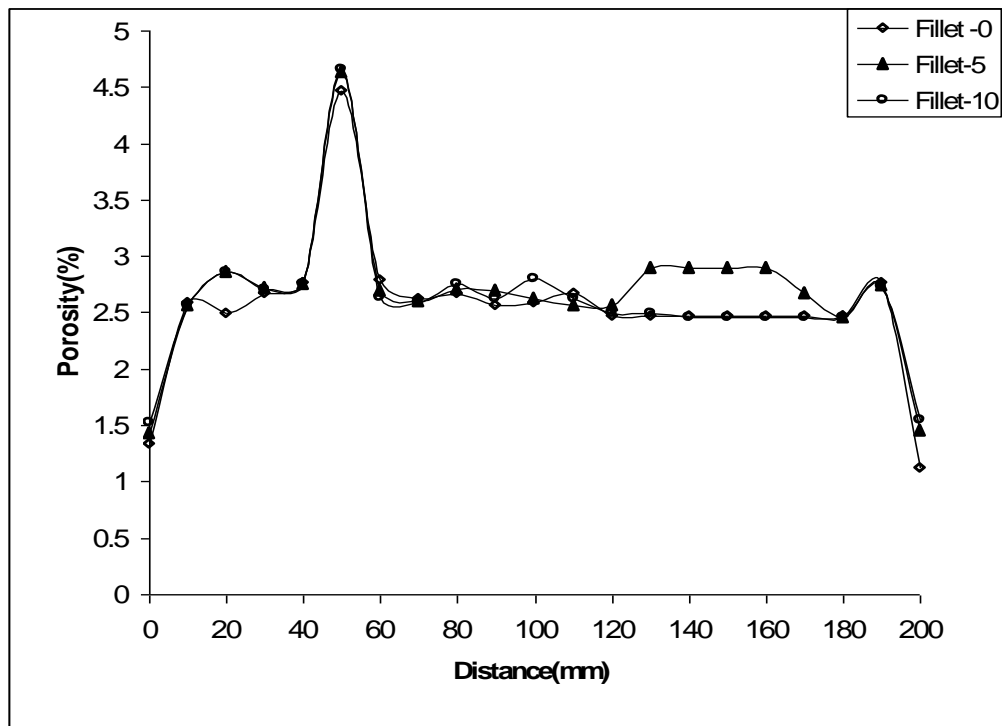


Fig. 5.5 Effect of fillet radius on porosity values along X-axis.

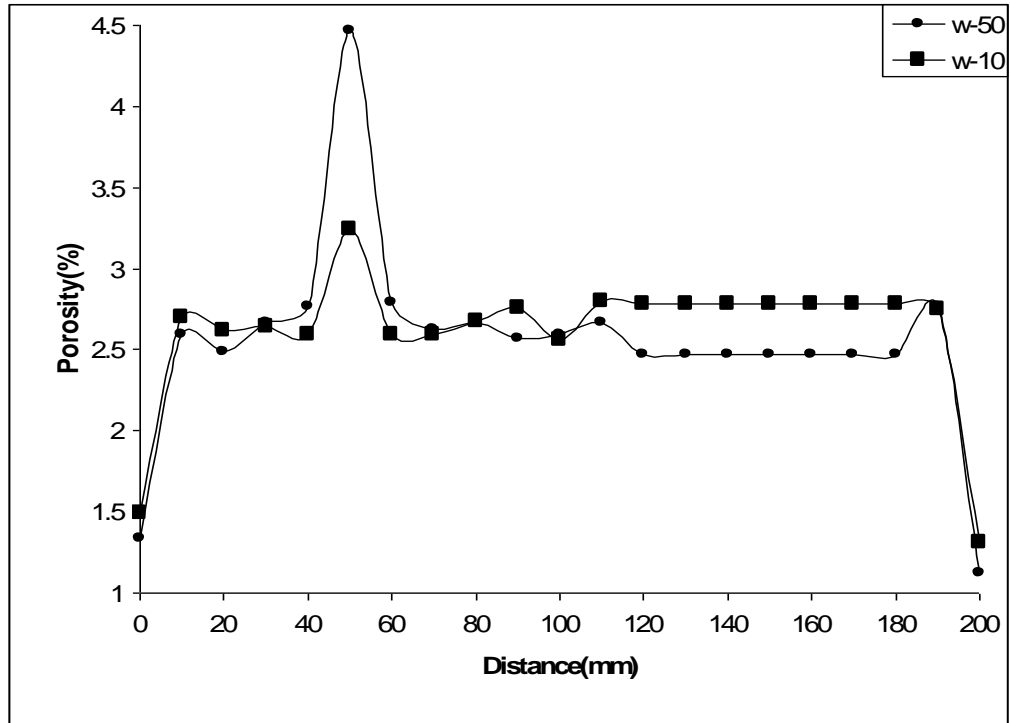


Fig. 5.6 Effect of width on porosity values along X-axis.

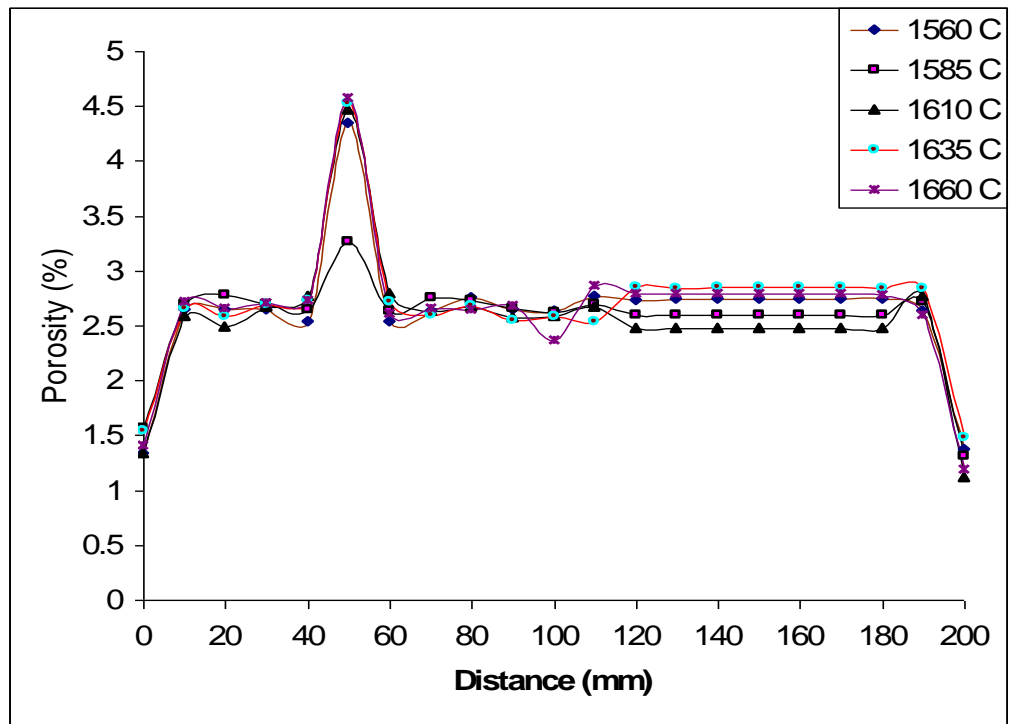


Fig. 5.7 Effect of pouring temperature on porosity values along X-axis.

5.2 Simulation Experiments

Based on preliminary simulation experiments with NovaSolid, the experiments were redesigned to conduct the simulations with MAGMAsoft and SIMULOR. This section describes the details about these simulations.

5.2.1 Material Details

Cast Metal: GS 16 Mn 5

Description: Low alloyed steel with 0.16 % C and 1.25 % Mn

Latent heat: 257 KJ/Kg

Solidus Temperature: 1442⁰ C Liquidus Temperature: 1510⁰ C

Properties like thermal conductivity, density and specific heat with different values of temperatures are given in Table 5.3.

Table 5.3: Properties of material.

Temperature (⁰ C)	Thermal Conductivity (W/m K)	Density (Kg/m ³)	Specific Heat (J/Kg K)
1	47.3	7849	451
50	47.1	7840	470
100	46.7	7825	503
200	45.5	7792	543
300	43.7	7757	577
500	38.3	7683	688
1000	28.72	7540	628
1200	30.52	7439	640
1400	32.3	7338	697
1442	32.7	7317	697
1510	30	7016	780
2000	30	6635	780

Mold material : Green sand

Initial temperature : 40⁰C

Sand : Bentonite : Water =100 : 7 : 4

Density : 1500 Kg/m³

5.2.2 Critical points in the geometry

The details of geometry used for the simulations are shown in Fig. 5.1 and picture of the model prepared in ProEngineer is shown in Fig. 5.2. After doing one or two preliminary simulations and by analysing the geometry critical points in the casting are identified. The Fig. 5.8 shows the position of critical points in sample casting. Table 5.4 gives the co-ordinates of the respective points.

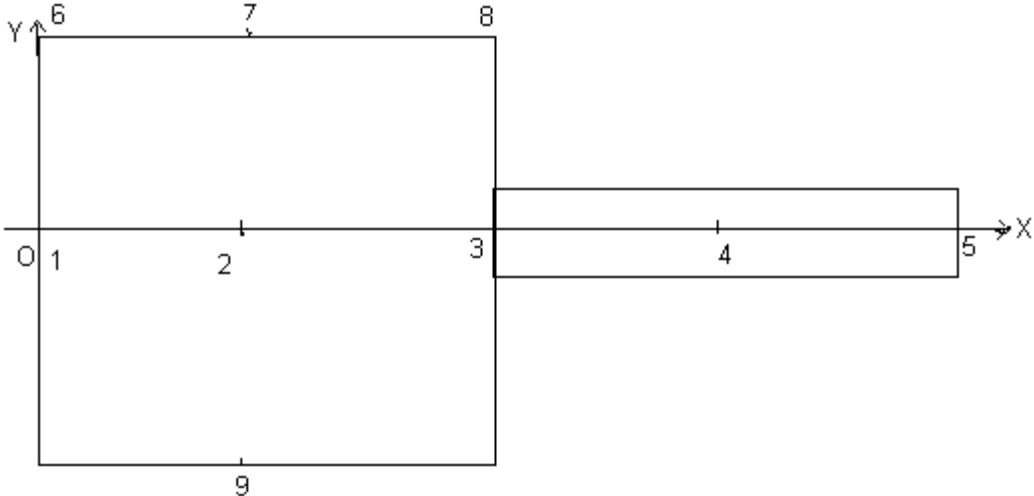


Fig. 5.8 Critical points in the sample geometry (Section at the middle).

Table 5.4: Co-ordinates of critical points

Points	1	2	3	4	5	6	7	8	9
X (mm)	0	50	100	150	200	0	50	100	50
Y (mm)	0	0	0	0	0	50	50	50	-50
Z (mm)	0	0	0	0	0	0	0	0	0

5.2.3 Structure of simulation sheet

To note the simulation details a sheet is designed which contains the description of simulation parameter, and results of simulation. The simulation sheet is same for MAGMAsoft and SIMULOR, only change is in case of MAGMAsoft percentage shrinkage is obtained from simulation whereas it is input in case of SIMULOR. Fig.5.9 shows the structure of simulation sheet.

No: 1

Title: Test1

Version: V 0

Parameter: Pouring Temperature

Parameter value: 1610 °C.

Results of simulations:

X(mm)	Temperature(°C.)	Time(s)	Porosity(%)
0			5.8
10	1425	965	
20	1430	1010	
30	1435	1020	
40	1440	1034	
50	1440	1031	40.6
60	1425	1007	
70	1415	950	
80	1410	900	
90	1375	675	6.0
100	1338	380	
110	1250	220	
120	1145	174	
130	1094	163	
140	1010	153	
150	925	149	6.0
160	890	147	
170	838	143	
180	790	132	
190	760	116	
200	735	116	5.9

Porosity: at 6 = 25.0 %, at 7 = 85.0 %, at 8 = 25.0 %, at 9 = 6.0 %

Total solidification time : 1109 s

Percentage shrinkage : 5.32 %

Fig. 5.9 Simulation sheet to note the results of simulation.

5.2.4 Design of Experiments

The design of experiments adopted for MAGMASoft is shown in Table 5.5 and Table 5.6 shows the design of experiments adopted for SIMULOR. Table 5.7 shows the sensitivity analysis structure for MAGMASoft and Table 5.8 shows the sensitivity analysis structure for SIMULOR

Table 5.5: Design of Experiments for MAGMASoft.

Simulation No.	Length mm	Fillet mm	Heat Transfer Coeff. W/m ² K	Feeding Effectivity %	Pouring Temperature °C
1	100	0	100	50	1610
2	125	0	100	50	1610
3	150	0	100	50	1610
4	100	5	100	50	1610
5	100	10	100	50	1610
6	100	0	1	50	1610
7	100	0	10	50	1610
8	100	0	100	30	1610
9	100	0	100	70	1610
10	100	0	100	50	1560
11	100	0	100	50	1585
12	100	0	100	50	1635
13	100	0	100	50	1660

Table 5.6: Design of Experiments for SIMULOR.

Simulation No.	Mass Feeding	Critical Solid Fraction Ratio	Heat Transfer Coeff. W/m ² K	Percentage Shrinkage %	Pouring Temperature °C
14	0.1	0.5	100	5	1610
15	0.2	0.5	100	5	1610
16	0.3	0.5	100	5	1610
17	0.1	0.3	100	5	1610
18	0.1	0.7	100	5	1610
19	0.1	0.5	1	5	1610
20	0.1	0.5	10	5	1610
21	0.1	0.5	100	4.5	1610
22	0.1	0.5	100	5.5	1610
23	0.1	0.5	100	5	1560
24	0.1	0.5	100	5	1585
25	0.1	0.5	100	5	1635
26	0.1	0.5	100	5	1660

Table 5.7: Sensitivity analysis for MAGMAsoft.

Simulation no:	Sensitivity analysis for:
1,2,3	Length
1,4,5	Fillet Radius
1,6,7	Heat Transfer Coefficient
1,8,9	Feeding Effectivity
1,10,11,12,13	Pouring Temperature

Table 5.8: Sensitivity analysis for SIMULOR.

Simulation no:	Sensitivity analysis for:
14, 15,16	Mass Feeding
14,17,18	Critical solid Fraction ratio
14,19,20	Heat Transfer Coefficient
14,21,22	Percentage Shrinkage
14,23,24,25,26	Pouring Temperature

CHAPTER 6

SENSITIVITY ANALYSIS MODEL

6.1 Introduction

This chapter describes the methodology and the tools developed for the analysis of simulation results. To compare the simulation runs in terms of porosity at a number of specified locations, it is required to obtain a single weighted value of porosity. For this purpose, weights were given to different locations based on their importance, determined using Analytic Hierarchy Process [18]. This is followed by development of two sensitivity analysis models using Microsoft Excel. Basic model gives the effect of a parameter on the different results of simulations. Advanced model performs the sensitivity analysis of parameters. The overall picture of analysis of simulation is shown in Fig. 6.1. The figure explains the stepwise procedure for doing the analysis. It include geometry evaluation, design of experiment to generate the sets of parameters for the simulation (Part A) and sensitivity analysis model which gives the sensitive and important parameters. Various steps in the procedure are described in detail next.

6.2 Weight assignment using AHP

The Analytic Hierarchy Process (AHP), a decision-aiding tool developed by Satty for complex and multi-attribute problems, can be used in the work to determine the relative weights to selection criteria [18]. The various steps to find the vector of weights and check the consistencies of judgement as suggested by Satty are as listed below.

- Construct a pair wise comparison matrix: Assuming n criteria, the pair wise comparison of criterion i with criterion j yields a square matrix of criteria called $A1_{n \times n}$. Where, a_{ij} is the element in the pair wise comparison matrix, giving comparative importance of criterion i with respect to criterion j. In matrix A1, $a_{ij} = 1$, when $i = j$ and $a_{ji} = 1/ a_{ij}$.

$$A1_{n \times n} = \begin{bmatrix} a_{11} & a_{12} & \dots & a_{1n} \\ a_{21} & a_{22} & \dots & a_{2n} \\ \dots & \dots & \dots & \dots \\ a_{n1} & a_{n2} & \dots & a_{nn} \end{bmatrix}$$

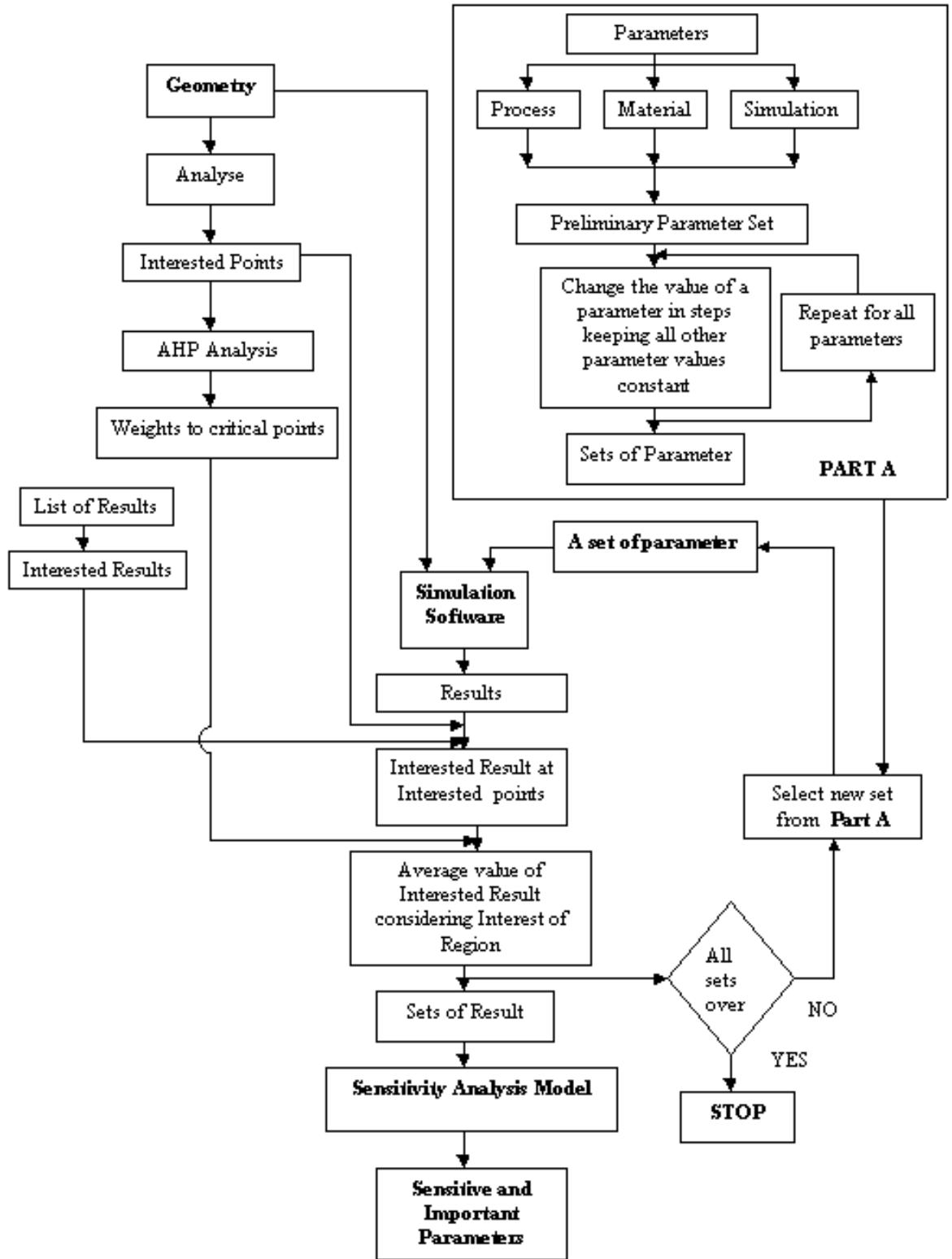


Fig. 6.1 Flowchart showing the overall process of analysis.

- Find weight of each criterion (W_j) by (a) Calculating geometric mean of i^{th} row (GM_i) and (b) then obtain the relative weights of each criterion by normalizing geometric means of rows in the comparative matrix.

$$GM_i = \left[\prod_{j=1}^n a_{ij} \right]^{1/n} \quad \text{and} \quad W_j = GM_i / \sum_{i=1}^n GM_i$$

- Calculate matrix $A3$ and $A4$, such that $A3 = A1 * A2$ and $A4 = A3 / A2$, where, $A2 = [W_1, W_2, \dots, W_n]^T$
- Find out the maximum eigen value (λ_{\max}), which is the average of matrix $A4$.
- Calculate consistency index (CI) = $(\lambda_{\max} - n) / (n-1)$.
- Obtain the random index (RI) from table 6.2, which is given by Satty for the number of criteria used in decision making.
- Finally, calculate the consistency ratio (CR) = CI / RI . Usually, a CR of 0.10 or less is considered acceptable.

Table 6.1: Scale of relative importance

Relative Importance (a_{ij})	Definition
1	Equal importance of i and j
3	Weak importance of i over j
5	Strong importance of i over j
7	Very strong importance of i over j
9	Absolute importance of i over j
2, 4, 6, 8	Intermediate values

Table 6.2: Random consistency Index table (RI)

Matrix order (n)	1	2	3	4	5	6	7	8	9	10
Random Index (RI)	0	0	0.58	0.9	1.12	1.24	1.32	1.41	1.45	1.49

While doing the analysis of the fin attached with a cube (test piece), results at the regions like center of the cube, center of the fin are more critical where as the result at the bottom of the cube is not important. So using AHP the more weights can be assigned for the center point and for the center of the fin, and less weight for bottom point of the cube.

Use of AHP approach to assign the weights provides following benefits:

- Gives average effect of a parameter on the simulation result of a casting, taking into account the user's region of interest.
- Doing such analysis software analyst will come to know which parameters are more important to achieve a specified task in the region of interest.

6.3 Basic Model

This model is developed to visualize the effect of a particular parameter on the different results of simulations. Using this model, the effect of parameters such as heat transfer coefficient, feeding effectivity, (which have to be provided by the user based on his experience) can be studied on the experiments of simulation. The model shows the variations of simulation results with a particular parameter. This model is developed using Microsoft Excel and it comprises the following seven sheets.

Sheet 1-5

Each sheet contains the details about a single simulation with particular value of parameter. Figure 6.2 shows sheet for feeding effectivity with value 30. The user has to enter the things like name of the software and parameter and (only in sheet1), value of parameter, times, temperatures, porosity values, percentage shrinkage and total solidification time. The *Italic* font is used for the input. From the entered data following graphs are generated in each cel sheet: (1) Temperature-Distance (2) Time-Distance (3) Gradient-Distance (4) Porosity-Distance. The sheet also gives the values of minimum gradient, maximum porosity and minimum porosity.

Software	<i>MAGMASoft</i>				
Parameter	<i>Effectivity</i>				
Value	<i>30</i>				
Distance	<i>Time</i>	<i>Temperature</i>	<i>Gradient</i>	<i>Porosity</i>	
0				<i>5.6</i>	
10	<i>1020</i>	<i>1420</i>	8		
20	<i>1064</i>	<i>1428</i>	1		
30	<i>1077</i>	<i>1429</i>	2		
40	<i>1085</i>	<i>1431</i>	1		
50	<i>1082</i>	<i>1430</i>	5	<i>78.8</i>	
60	<i>1050</i>	<i>1425</i>	25		
70	<i>995</i>	<i>1400</i>	5		
80	<i>942</i>	<i>1395</i>	25		
90	<i>740</i>	<i>1370</i>	35		Percent Shrinkage(%) <i>5.325</i>
100	<i>500</i>	<i>1335</i>	95	<i>5.6</i>	Total Solidification Time(s) <i>1109</i>
110	<i>226</i>	<i>1240</i>	110		Min. Gradient(^o C/mm) <i>1</i>
120	<i>176</i>	<i>1130</i>	51		Max. Porosity(%) <i>78.8</i>
130	<i>165</i>	<i>1079</i>	97		Min. Porosity(%) <i>5.6</i>
140	<i>155</i>	<i>982</i>	43		
150	<i>153</i>	<i>939</i>	74	<i>5.6</i>	
160	<i>149</i>	<i>865</i>	60		
170	<i>142</i>	<i>805</i>	20		
180	<i>138</i>	<i>785</i>	35		
190	<i>124</i>	<i>750</i>	15		
200	<i>115</i>	<i>735</i>		<i>5.6</i>	

Fig. 6.2 Typical picture of sheet 1 of basic model.

Sheet 6

The Figure 6.3 shows a portion of sheet 6 to calculate the weights to critical locations in the castings. User has to enter the name of result and fill the *Italic* font values of table with the weights by pair wise comparison. Column *G.M.* shows geometric means of rows and the column *Weights* gives the calculated weight for each location.

Parameter	<i>Effectivity</i>		Result Type		<i>Porosity</i>						
	1	2	3	4	5	6	7	8	9	G.M	Weights
1	1.0	<i>0.2</i>	<i>0.2</i>	<i>0.2</i>	<i>0.3</i>	<i>0.3</i>	<i>0.2</i>	<i>0.3</i>	<i>3.00</i>	0.38	3.2
2	5.0	1.0	<i>1.0</i>	<i>1.0</i>	<i>3.0</i>	<i>5.0</i>	<i>1.0</i>	<i>5.0</i>	<i>9.0</i>	2.47	20.6
3	5.0	1.0	1.0	<i>1.0</i>	<i>3.0</i>	<i>3.0</i>	<i>1.0</i>	<i>3.0</i>	<i>8.0</i>	2.17	18.1
4	5.0	1.0	1.0	1.0	<i>3.0</i>	<i>3.0</i>	<i>1.0</i>	<i>3.0</i>	<i>8.0</i>	2.17	18.1
5	3.0	0.3	0.3	0.3	1.0	<i>1.0</i>	<i>0.3</i>	<i>1.0</i>	<i>5.0</i>	0.83	6.9
6	3.0	0.2	0.3	0.3	1.0	1.0	<i>0.3</i>	<i>1.00</i>	<i>5.0</i>	0.78	6.5
7	5.0	1.0	1.0	1.0	3.0	3.0	1.0	<i>3.0</i>	<i>9.0</i>	2.20	18.4
8	3.0	0.2	0.3	0.3	1.0	1.0	0.3	1.0	<i>5.0</i>	0.78	6.5
9	0.3	0.1	0.1	0.1	0.2	0.2	0.1	0.2	1.0	0.20	1.7
										0.12	100.0
										Index	0.044
										Ratio	0.03

Fig. 6.3 Weight assignment to critical points using AHP.

Sheet 7

This sheet is automatically generated using the values from sheets 1 to 6. This sheet contains six graphs (Fig. 6.4), which describe the effect of change in parameter on following:.

- Total solidification time (Graph A).
- Minimum gradient in the casting (Graph B).
- Minimum porosity in the casting (Graph C).
- Maximum porosity in the casting (Graph D).
- Percentage shrinkage of the casting (Graph E).
- Porosity calculated using AHP (Graph F).

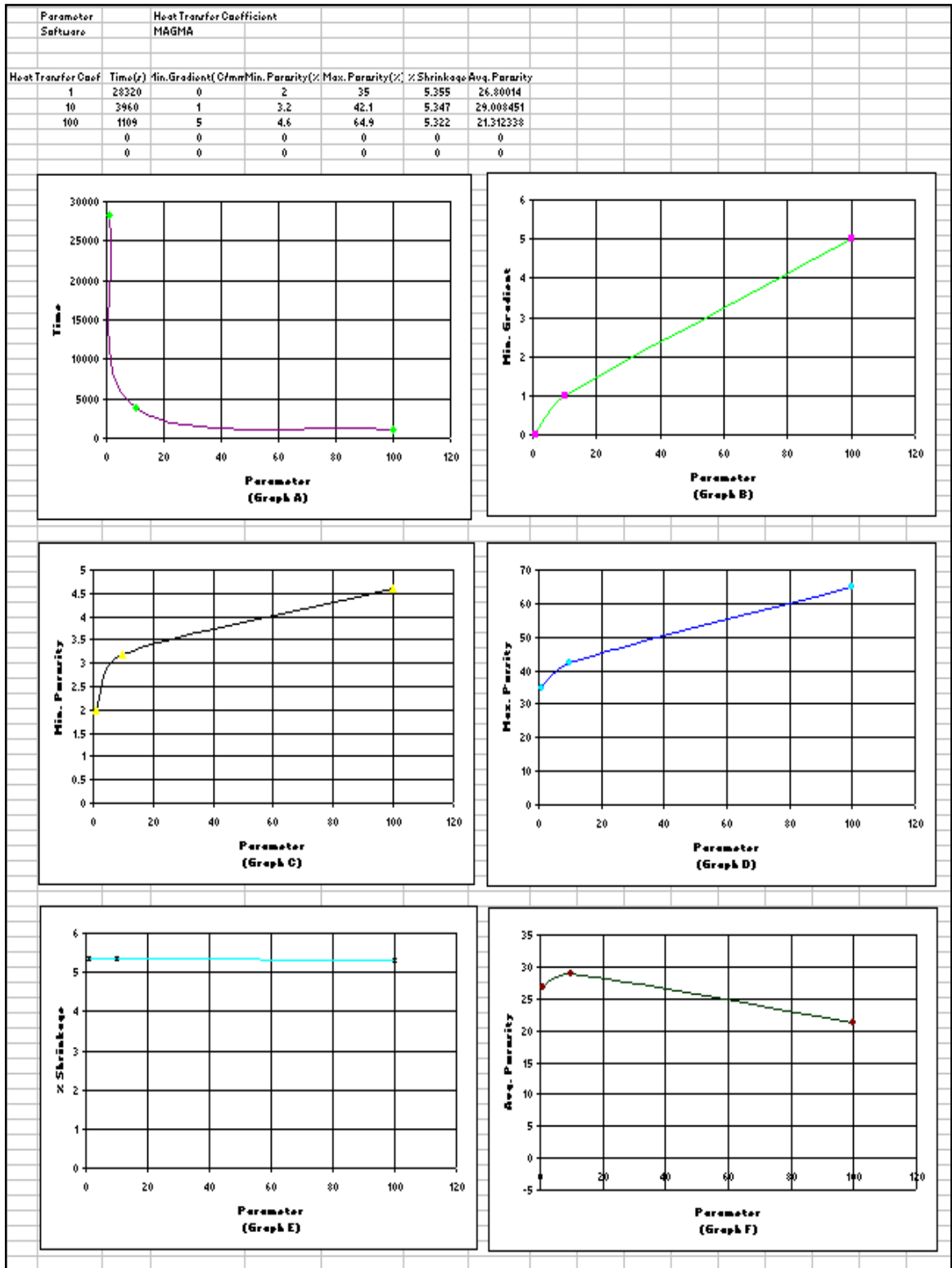


Fig. 6.4 Picture showing result sheet of basic model.

6.4 Advanced Model

This model analyses the importance and sensitiveness of the parameters under study. The model is developed in Microsoft Excel for a maximum of six parameters. The flowchart of the model is given in Fig. 6.5. This analysis will help to find the critical parameters of simulation software for a particular result. This model comprises following seven sheets.

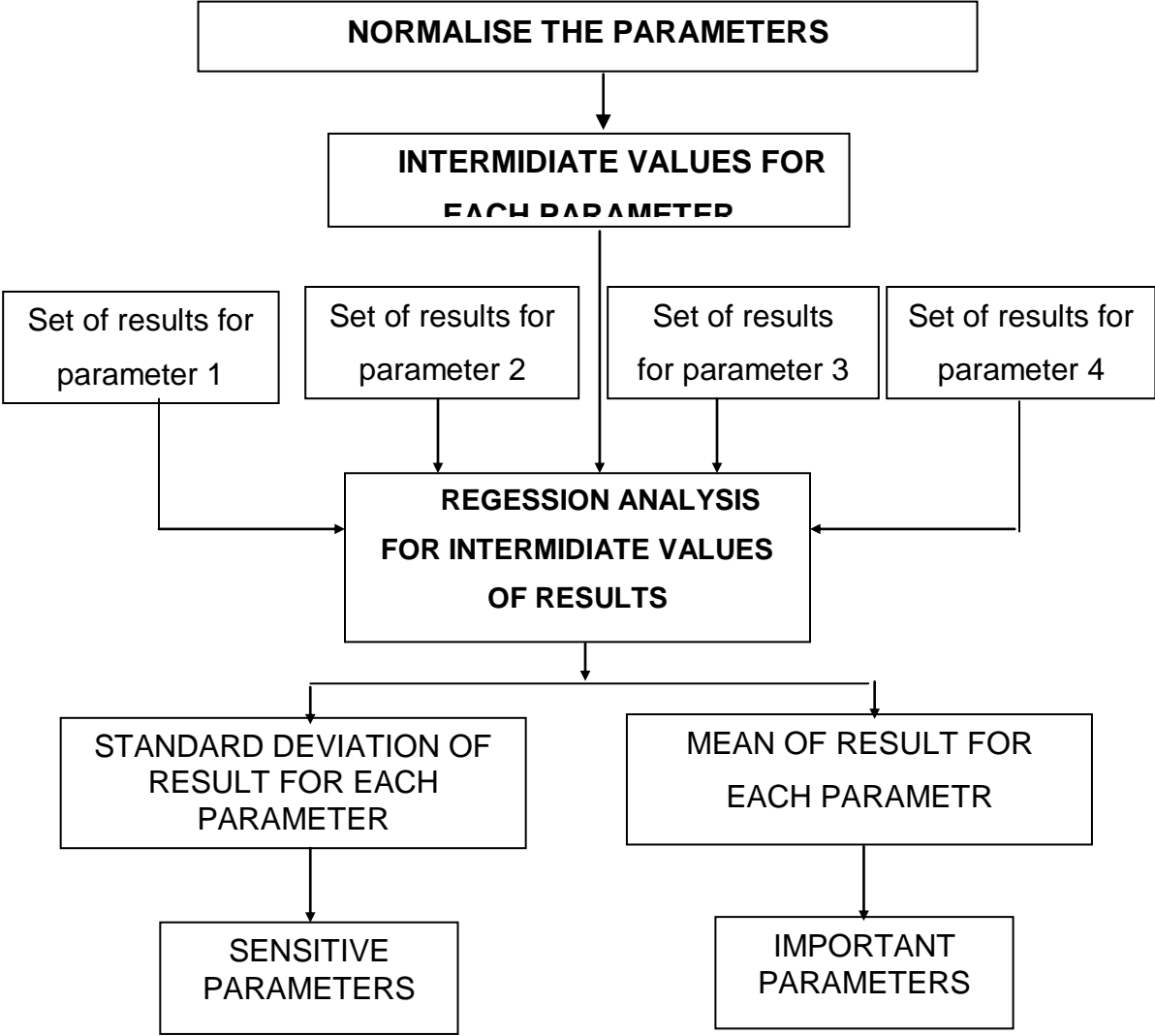


Fig. 6.5 Flowchart of advanced model for sensitivity analysis.

Sheet 1 (Fig. 6.6)

This sheet contains contents of the model and color code used in the model.

SENSITIVITY ANALYSIS MODEL	
INTRODUCTION	
SHEET 1	INTRODUCTION / COLOUR CONVENTION
SHEET 2	GENERAL INPUT
SHEET 3	AHP ANALYSIS
SHEET 4	INPUT
SHEET 5	NORMALISATION OF PARAMETERS
SHEET 6	CALCULATIONS USING REGRESSION ANALYSIS
SHEET 7	QUANTITATIVE RESULTS
SHEET 8	QUALITATIVE RESULTS
COLOUR CONVENTIONS	
COLOUR	TITLES
COLOUR	INPUT
COLOUR	INSTRUCTION / WARNINGS
COLOUR	SUB-TITLES
COLOUR	RESULTS
COLOUR	NORMAL

Fig. 6.6 Picture showing sheet 1 of advanced model.

Sheet 2: This sheet contains the general input like name of the software, name of result, minimum and maximum values of the result and some instructions to proceed further (Fig. 6.7).

GENERAL INPUT				
Name of Software	MAGMAsoft			
Result No.	1			
Result Name	Average Porosity			
Minimum	0			
Maximum	100			
Expected Result Max(Yes=1)	2			
AHP Analysis (Yes=1)	1			Go to Sheet 3

Fig. 6.7 Picture showing the sheet 2 of advanced model.

Sheet 3: This sheet can be used if values of the results are different at different points in the casting for a single parameter. The nine critical points in the casting are analysed and then results are noted at these points. The weights are assigned to each point using Analytical Hierarchy Process. The different weights can be assigned to each point depending on the interest of the point. The maximum nine points can be compared. Calculation of weights is by pair wise comparison between two points.

ANALYTICAL HIRECHICAL PROCESS																
Prameter No.	1	Parameter	Superheat		No. of Sim		5				Res1	Res2	Res3	Res4	Res5	
1	1.0	2	3	4	5	6	7	8	9	G.M	Weights	50	75	100	125	150
2	0.2	0.2	0.2	0.3	0.3	0.2	0.3	3.0	0.383	3.19	10.00	10.00	10.00	10.00	10.00	
3	5.0	1.0	1.0	1.0	3.0	5.0	1.0	5.0	2.466	20.56	100.00	100.00	100.00	100.00	100.00	
4	5.0	1.0	1.0	1.0	3.0	3.0	1.0	3.0	2.173	18.12	10.00	10.00	10.00	10.00	10.00	
5	5.0	1.0	1.0	1.0	3.0	3.0	1.0	3.0	2.173	18.12	10.00	10.00	10.00	10.00	10.00	
6	3.0	0.3	0.3	0.3	1.0	1.0	0.3	1.0	0.829	6.91	10.00	10.00	10.00	10.00	10.00	
7	3.0	0.2	0.3	0.3	1.0	1.0	0.3	1.0	0.783	6.53	10.00	10.00	10.00	10.00	10.00	
8	5.0	1.0	1.0	1.0	3.0	3.0	1.0	3.0	2.202	18.36	20.00	10.00	20.00	10.00	10.00	
9	3.0	0.2	0.3	0.3	1.0	1.0	0.3	1.0	0.783	6.53	10.00	10.00	10.00	10.00	10.00	
9	0.3	0.1	0.1	0.1	0.2	0.2	0.1	0.2	0.200	1.67	10.00	10.00	10.00	10.00	10.00	
										0.120	100.00					
Value of Average Parameter												30.34	28.51	30.34	28.51	28.51
PROCEED FUTHER																

Fig. 6.8 AHP used to calculate average porosity for the superheat parameter.

In Fig. 6.8 the inputs are represented with bold font. The first 10 by 10 part of the table is the pair wise comparison of the points. The procedure is as follows (Table 6.1):

Cell1=1 ;

Point 1 is equally important as point 1.

Cell2=0.2;

Point 1 is 1/5(=0.2) times important than 2 (Or Point 2 is 5 times important than Point1). Similarly, Point 1 is 1/5(=0.2) times important than 3, Point 1 is 1/5(=0.2) times important than 4, Point 1 is 1/3(=0.3) times important than 5, Point 1 is 1/3(=0.3) times important than 6, Point 1 is 1/5(=0.2) times important than 7, Point 1 is 1/3(=0.3) times important than 8, Point 1 is 3 times important than 9.

After entering all bold font values, weight for each location is displayed in column *Weight*. The values of the results are entered in the corresponding parameter value columns. The row *Value of Average Parameter* shows the single valued result corresponding to parameter value.

At the bottom in the Fig. 6.8 an instruction *PROCEED FURTHER* appears which confirm the validity of assigned weights by AHP. If assigned weights violate the theory of AHP, then instruction will be as *REASSIGN WEIGHTS*.

Sheet 4 : This sheet is used only if the values of the results are single valued like total solidification time. This sheet is alternative for the sheet 3 and used only if the results are not calculated from AHP. In this sheet one has to enter the parameter name, no of simulations carried (≥ 3), parameter values and corresponding result values (Fig. 6.9).

Parameter No.	1
Parameter	Superheat
No. Of Simulations	5
Parameter values	Result
50	960
75	1021
100	1109
125	1183
150	1254

Fig. 6.9 Input format for single valued result.

Sheet 5: This sheet is used for the normalization of parameters. For analysis, results corresponding to all parameters should be compared on the common ground. So all parameters are normalized between 0 and 1. If user gives choice as *1* for variable *Linear*, then instruction *ENTER MIN AND MAX VALUE* will occur, and after entering these values parameter is normalized in minimum and maximum value in the linear law (Fig. 6.10). For other law user has to enter all intermediate values in the column *Manual*. A graph is also provided to see the variations of parameter in the minimum and maximum value (Fig. 6.7). The instruction *PROCEED FURTHER* will occur if the constraints and further calculation are possible for the range. The instruction *DATA INSUFFICIENT* will occur if it is not possible to predict the further result from the given calculations. The remedy for this is to carry more simulations in the range or to reduce the range.

Parameter No	1			
Parameter	Superheat		Linear	Manual
No. of simulation	5		0	20
			0.1	15
			0.2	18
			0.3	24
Parameter values	Result		0.4	38
50	4.719		0.5	50
75	5.029		0.6	70
100	5.322		0.7	90
125	5.579		0.8	120
150	5.835		0.9	150
Slope	20		1	220
Linear(Y=1)	2		ENTER VALUES IN COL MANUAL	
Minimum	20			
Maximum	220			
				PROCEED

Fig. 6.10 Normalization of parameters.

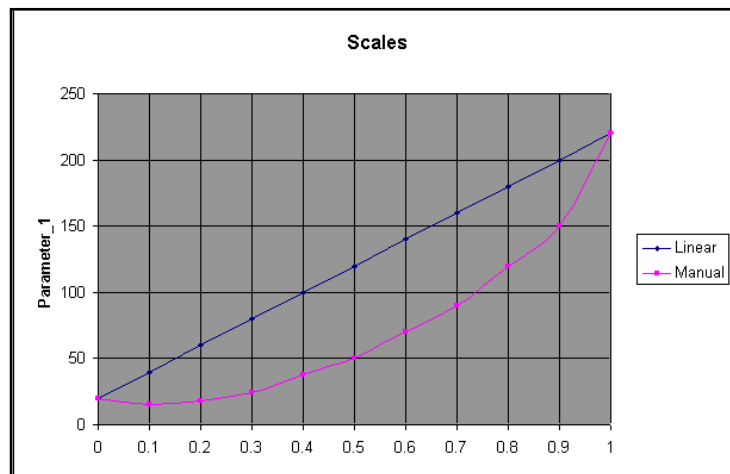


Fig. 6.11 Graph to see the variations in between minimum and maximum value.

Sheet 6

This sheet is the calculation sheet and no value is needed to be entered.

Sheet 7

Sheet 7 is for the results of sensitivity analysis. The picture of sheet is shown in Fig. 6.12. The sheet includes the name of software and result name. The sheet gives the percentage sensitiveness and percentage importance the parameter. The same is also presented in the graphical way. Column *Correlation* gives whether parameter has increasing or decreasing effect on the result value. The value 1 represents increasing value of the result with increase in parameter value. The -1 value represents the decreasing value with increase in parameter value. The value 0 represents no effect of parameter on result.

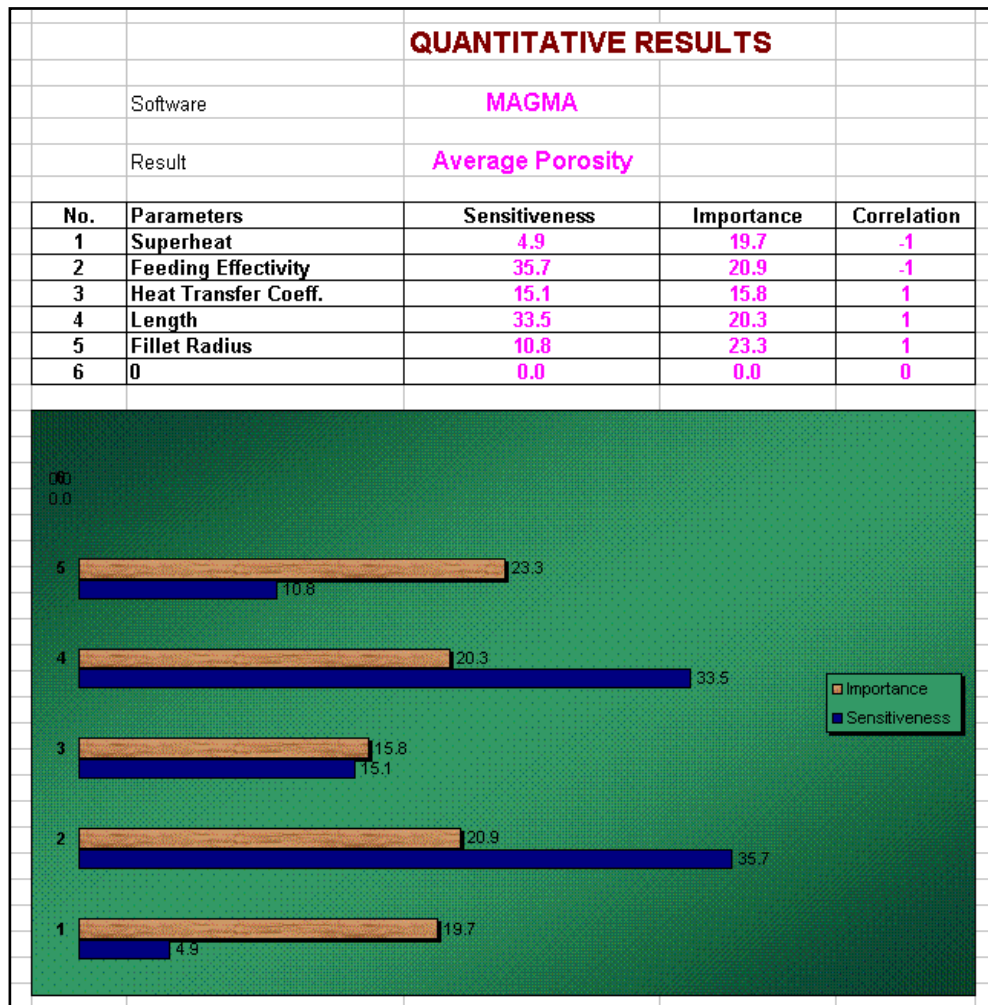


Fig. 6.12 Picture of sheet 7 showing results of analysis.

CHAPTER 7

RESULTS AND ANALYSIS

7.1 Results

Basic model gives the effect of a parameter on different results of simulation. The Table 7.1 summarises all the results obtained from basic model. Figure 7.1 shows the screen print of result with MAGMAsoft for the study object. Figure 7.2 shows the screen print of shrinkage result with SIMULOR for the study object. The Table 7.2 shows the results obtained from advanced model.

Table 7.1: Summary of results of basic model.

Parameters (Range)	Software	Solidification Time s	Min. Gradient °C/mm	Min. Porosity %	Max. Porosity %	Percentage Shrinkage %	Avg. Porosity %
Heat Transfer Coefficient 1-100 W/m ² K	MAGMAsoft	1109 - 28320	0 - 5	2 - 4.6	35 - 64.9	7.322 - 7.355	21.31 - 29.00
	SIMULOR	2073 - 35309	0 - 1	10 - 10	100 - 100	7.000 - 7.000	27.55 - 31.04
Superheat 50-150 °C	MAGMAsoft	960 - 1254	0 - 5	4.6 - 7.6	64.9 - 97.6	4.719 - 7.835	21.78 - 29.00
	SIMULOR	1837 - 2387	1 - 1	10 - 10	100 - 100	7.000 - 7.000	28.51 - 30.34
Feeding Effectivity 30 - 70	MAGMAsoft	1109 - 1109	1 - 5	4.6 - 7.6	64.9 - 89.5	7.322 - 7.355	21.31 - 37.57
Cr. Solid Fraction 0.3 - 0.7	SIMULOR	2073 - 2073	1 - 1	10 - 10	100 - 100	7.000 - 7.000	30.34 - 47.03
End of Mass Feeding 0.1-0.3	MAGMAsoft	-	-	-	-	-	-
	SIMULOR	2073 - 2073	1 - 1	10 - 10	100 - 100	7.000 - 7.000	30.34 - 36.77
Percentage Shrinkage 4.5-7.5	MAGMAsoft	-	-	-	-	-	-
	SIMULOR	2073 - 2073	1 - 1	10 - 10	100 - 100	4.500 - 7.500	30.34 - 33.46
Length 100 - 150 mm	MAGMAsoft	1096 - 1109	1 - 5	4.6 - 7.4	64.9 - 90.5	7.317 - 7.322	26.31 - 33.08
	SIMULOR	-	-	-	-	-	-
Fillet Radius 0-10 mm	MAGMAsoft	990 - 1109	0 - 5	4.6 - 7.8	64.9 - 97.0	7.322 - 7.324	21.31 - 36.65
	SIMULOR	-	-	-	-	-	-

Table: 7.2 Results from advanced model.

Result type	Parameters	Sensitiveness*		Importance*	
		MAGMASoft	SIMULOR	MAGMASoft	SIMULOR
Total solidification time	Heat transfer coefficient	96.9	96.5	69.0	57.7
	Superheat	2.5	3.5	8.2	11.0
	Feeding effectivity	0.0	0.0	7.8	10.4
	End of mass feeding	-	0.0	-	10.4
	Percentage shrinkage	-	0.0	-	10.4
	Length	0.2	-	7.7	-
	Fillet radius	0.4	-	7.3	-
Average porosity	Heat transfer coefficient	15.1	1.4	15.8	17.8
	Superheat	4.9	2.4	19.7	17.2
	Feeding effectivity	35.7	27.5	20.9	21.3
	End of mass feeding	-	20.0	-	23.5
	Percentage shrinkage	-	48.7	-	20.2
	Length	33.5	-	20.3	-
	Fillet radius	10.8	-	23.3	-

* Please note that values of sensitiveness and importance are normalized among the parameters available for the particular software.

7.2 Conclusions

The conclusions of the results obtained from basic model are summarised in Table 7.3. Parameters are relatively more sensitive to results in case of MAGMASoft than SIMULOR.

From the Table 7.2 it can be seen that for the total solidification time heat transfer coefficient is critical (sensitive and important) for both the software packages. However for the average porosity, in case of MAGMASoft the critical parameter is feeding effectivity (Or critical solid fraction ratio). In case of SIMULOR most sensitive is the percentage shrinkage and most important is end of mass feeding. The conclusions are summarised in Table 7.4.

Table 7.3: Conclusions from the results of basic model.

Parameters	Software	Effect on	No effect on
Heat Transfer Coefficient	M	Total solidification time Minimum gradient Minimum porosity, Maximum porosity Percentage shrinkage, Average porosity	-
	S	Total solidification time Minimum gradient Average porosity	Minimum porosity Maximum porosity Percentage shrinkage
Superheat	M	Total solidification time Minimum gradient Minimum porosity Maximum porosity Percentage shrinkage Average porosity	-
	S	Total solidification time Average porosity	Minimum gradient Minimum porosity Maximum porosity Percentage shrinkage
Feeding Effectivity (Cr. Solid Fraction)	M	Minimum gradient Minimum porosity Maximum porosity Percentage shrinkage Average porosity	Total solidification time
	S	Average porosity	Total solidification time Minimum gradient Minimum porosity Maximum porosity Percentage shrinkage
End of mass feeding	S	Average porosity	Total solidification time Minimum gradient Minimum porosity Maximum porosity Percentage shrinkage
Percentage Shrinkage	S	Average porosity Percentage shrinkage	Total solidification time Minimum gradient Minimum porosity Maximum porosity
Length	M	Total solidification time Minimum gradient Minimum porosity Maximum porosity Percentage shrinkage Average porosity	-
Fillet Radius	M	Total solidification time Minimum gradient Minimum porosity Maximum porosity Percentage shrinkage Average porosity	-

M – MAGMAsoft

S - SIMULOR

Table 7.4: Conclusions from the results of advanced model.

Result	Software	Most Sensitive	Most Important
Average porosity	MAGMASoft	Feeding effectivity	Length
	SIMULOR	Percentage shrinkage	End of Mass feeding
Solidification time	MAGMASoft	Heat transfer coefficient	Heat transfer coefficient
	SIMULOR	Heat transfer coefficient	Heat transfer coefficient

7.3 Customization

The process of customization for a software is necessary to match the actual results with the predicted results of simulations. The Fig. 7.3 shows the flowchart of the proposed customization process. The important activity for the customization includes the modification or the application of correction factors to the parameters. As this project has identified most sensitive and important parameters, the correction factors can be applied to only those parameters that are important or sensitive. This reduces the number of trials for the customization, which in turn lowers the time and expense for customization.

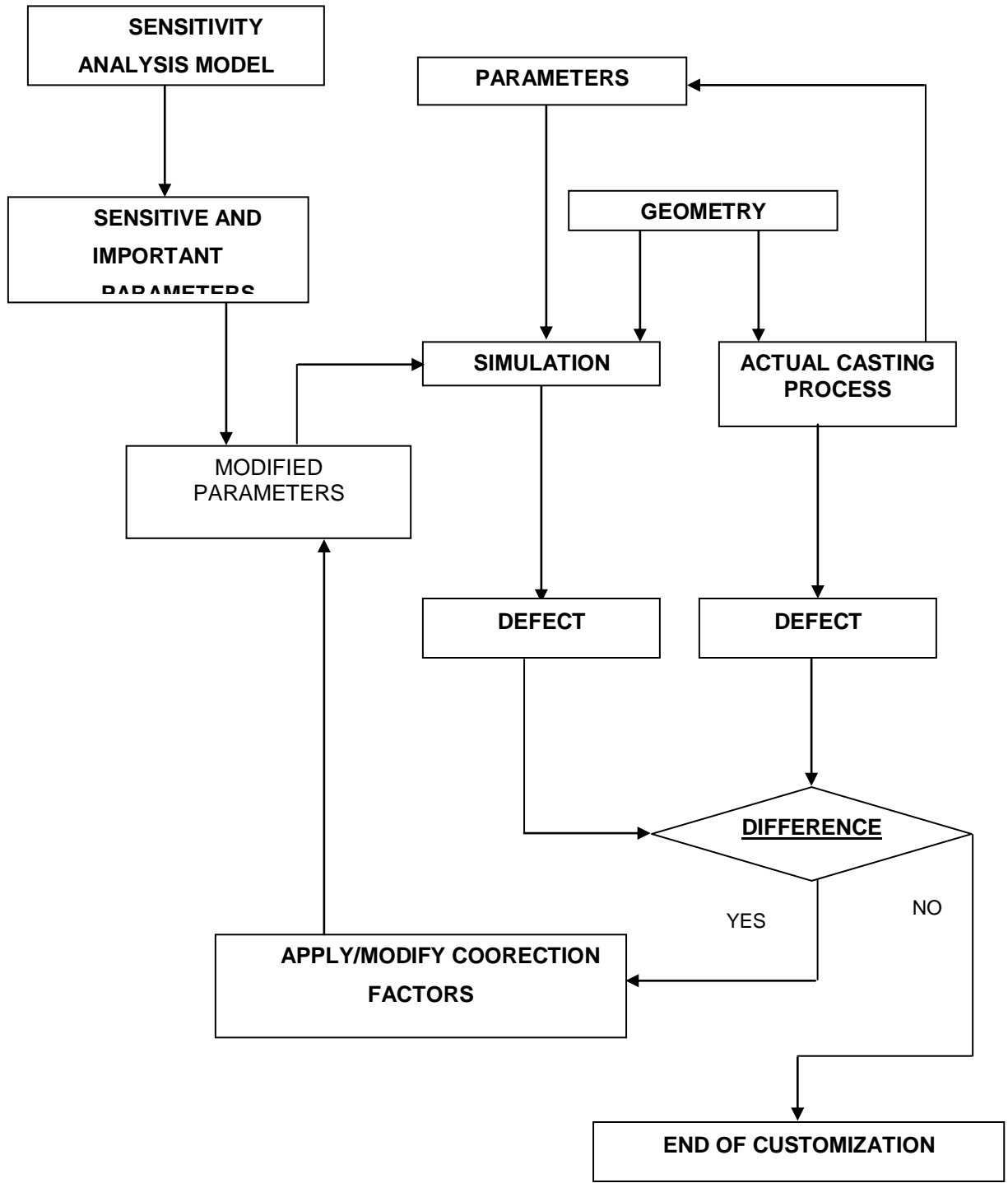


Fig. 7. 3 Proposed method for customization.

CHAPTER 8

CONCLUSIONS

8.1 Summary of work done

The work has been completed partly at Indian Institute of Technology Bombay, India and partly at the Centro Ricerche Fiat Turin, Italy. The important tasks of the work completed include:

- Literature review on heat transfer analysis, shrinkage prediction methods and implementation tools (finite difference method, finite element method and boundary element method).
- Learning the user interface of the following casting simulation software packages
 - 1) NovaSolid
 - 2) MAGMAsoft
 - 3) PAMCAST/SIMULOR.
- Preliminary simulation experiments with NovaSolid to learn the solidification simulation analysis and to design further analysis.
- Simulation experiments with MAGMAsoft.
- Simulation experiments with PAMCAST/SIMULOR.
- Development of sensitivity analysis models using Microsoft Excel.
- Sensitivity analysis of simulation results obtained from MAGMAsoft and SIMULOR.
- Evolution of customization approach for a software package according to a particular industry to match actual and predicted defects.

8.2 Conclusions of work done

Following conclusions can be made from the work completed:

- Results like minimum gradient, minimum porosity and maximum porosity are relatively more sensitive in case of MAGMAsoft than SIMULOR for parameters like heat transfer coefficient, superheat, and feeding effectivity.
- For the total solidification time heat transfer coefficient is critical (sensitive and important) for both the software packages.

- For the average porosity, in case of MAGMASoft the critical parameter is feeding effectivity In case of SIMULOR most sensitive is the percentage shrinkage and most important is end of mass feeding.
- There are some input parameters that do not affect particular results; these parameters can be ignored depending on results desired.
- Analytical Hierarchical Process approach gives relative importance to the points inside a casting, useful to optimize the value of result in the region of interest.
- For the same results of simulation, sensitive and important parameters for the two software packages may differ from each other.
- A fast and systematic approach for customization of software for a given organization is proposed which reduces the need for large number of trials.

REFERENCES

- [1] G. Upadhyaya and A.J. Paul, "Solidification Modelling: A Phenomenological Review", *AFS Transactions*, **102**,1994, pp. 69-80.
- [2] R.E. Marrone, J.O. Wilkes and R.D. Pehlke, "Numerical Simulation of Solidification Part-1: Low Carbon Steel Casting – 'T' shape", *Cast Metals Research Journal*, **6** (4), 1970, pp. 184-188.
- [3] H.L. Tsai, "Determination of Latent Heat Release and its Effect on Casting Solidification", *Proceedings of the Fifth International Conference on Modelling of Casting and Welding Processes*, (Edited by Michel Rappaz et. al), September 16-21, 1990, Davos, Switzerland, pp. 545-550.
- [4] R.E. Marrone, J.O. Wilkes and R. D. Pehlke, "Numerical Simulation of Solidification Part – II: Low Carbon Steel Casting – 'L' Shape", *Cast Metals Research Journal*, **6** (4), 1970, pp. 188-192.
- [5] E. Majchrzak and J. Mendakiewicz, "Numerical Analysis of Cast Iron Solidification Process", *Journal of Material Processing Technology*, **53** (1-2), 1995, pp. 285-292.
- [6] C.S. Wei and J.T. Berry, "Solidification Simulation Based on the Edge Function Approach", *AFS Transactions*, **91**, 1983, pp. 509-514.
- [7] I. Imafaku and K. Chijiiwa, "A Mathematical Model for Shrinkage Cavity Prediction in Steel Castings", *AFS Transactions*, **91**, 1983, pp. 527-537.
- [8] E. Niyama, T. Uchida, M. Morikawa and S. Saito, "Predicting Shrinkage in large Steel Castings from Temperature Gradient Calculations", *International Cast Metals Journal*, **6**(2), 1981, pp. 16-22.
- [9] S.J. Neises, J.J. Uicker and R.W. Heine, "Geometric Modelling of Directional Solidification Based on Section Modulus", *AFS Transactions*, **95**,1987, pp. 25-30.
- [10] R.M. Kotschi and L.A. Plutshack, "An Easy and Inexpensive Technique to Study the Solidification of Castings in Three Dimensions", *AFS Transactions*, **89**, 1981, pp. 601-610.
- [11] B. Ravi and M.N. Srinivasan, "Casting Solidification Analysis by Modulus Vector Method", *International Journal of Cast Metals Research*, **9**,1996, pp. 1-7.

- [12] B. Ravi and M.N. Srinivasan, "Hot Spots in Castings: Computer Aided Location and Experimental Validation", *AFS Transactions*, **98**,1990, pp. 353-357.
- [13] G. Vanhoutte, "Numerical Simulation of Casting Solidification: Application to the Sand-Coated Gravity Die Casting Process", *AGARD Conference Proceedings No. 325 on Advanced Casting Technology*, April 4-7, 1982, Brussels, Belgium, pp. 7.1-7.14.
- [14] R. D. Cook, D. S. Malkus and M. E. Plesha, *Concepts and Applications of Finite Element Analysis*, John Wiley and Sons, New York, 1989, pp. 1-4, 484-485.
- [15] R.W. Lewis, H.C. Huang, A.S. Usmani and M.R. Tadayan, "Solidification in Casting by Finite Element Method", *Material Science and Technology*, **6** (5), 1990, pp. 482-489.
- [16] T.X. Hou, R.D. Pehlke and J.O. Wilkes, "Computer Simulation of Casting Solidification Using a Combination of Finite Element and Boundry Element Methods", *Proceedings of the fifth International Conference on Modelling of Casting and Welding Processes*, (Edited by Michel Rappaz et. al), September 16-21, 1990, Davos, Switzerland, pp. 15-22.
- [17] G. Upadhya and A.J. Paul, "Comprehensive Casting Analysis Model Using a Geometry-Based Technique Followed by Fully Coupled, 3-D Fluid Flow, heat Transfer and Solidification Kinetics Calculations", *AFS Transactions*, **100**,1992, pp.925-933.
- [18] T. L. Satty, " How to make a decision: The Analytic Hierarchy Process", *European Journal of Operatations Research*, **48**, pp 9-26, 1990.